



HAL
open science

NatB-mediated N-terminal acetylation affects growth and biotic stress responses

Monika Huber, Willy V Bienvenut, Eric Linster, Iwona Stephan, Laura Armbruster, Carsten Sticht, Dominik C. Layer, Karine Lapouge, Thierry Meinnel, Irmgard Sinning, et al.

► **To cite this version:**

Monika Huber, Willy V Bienvenut, Eric Linster, Iwona Stephan, Laura Armbruster, et al.. NatB-mediated N-terminal acetylation affects growth and biotic stress responses. *Plant Physiology*, 2020, 182 (2), pp.792-806. 10.1104/pp.19.00792 . hal-02989528

HAL Id: hal-02989528

<https://hal.science/hal-02989528v1>

Submitted on 16 Nov 2020

HAL is a multi-disciplinary open access archive for the deposit and dissemination of scientific research documents, whether they are published or not. The documents may come from teaching and research institutions in France or abroad, or from public or private research centers.

L'archive ouverte pluridisciplinaire **HAL**, est destinée au dépôt et à la diffusion de documents scientifiques de niveau recherche, publiés ou non, émanant des établissements d'enseignement et de recherche français ou étrangers, des laboratoires publics ou privés.

1 **Short title:** NatB acetylates 20% of the proteome in Arabidopsis

2

3 **NatB-mediated N-terminal acetylation affects growth and abiotic stress**
4 **responses**

5

6 **One-sentence Summary:** Initiator methionine acetylation by NatB is evolutionary
7 conserved and critical for abiotic stress responses in *Arabidopsis thaliana*.

8

9 **Authors:**

10 Monika Huber¹, Willy V. Bienvenut², Eric Linster¹, Iwona Stephan¹, Laura
11 Armbruster¹, Carsten Sticht³, Dominik Layer⁴, Karine Lapouge⁴, Thierry Meinel²,
12 Irmgard Sinning⁴, Carmela Giglione^{2,*}, Ruediger Hell¹ and Markus Wirtz^{1,*}

13

14 **Authors affiliation:**

15 ¹Centre for Organismal Studies, Heidelberg University, 69120 Heidelberg, Germany.

16 ²Institute for Integrative Biology of the Cell (I2BC), CEA, CNRS, Université Paris-Sud,
17 Université Paris Saclay, 91198 Gif-sur-Yvette Cedex, ³Center for Medical Research,
18 Mannheim 68167, Germany. ⁴Heidelberg University Biochemistry Center, 69120
19 Heidelberg, Germany.

20

21 ***Corresponding authors:**

22 Markus Wirtz

23 Phone: +49-6221-54334, Fax: +49-6221-545859

24 E-mail: markus.wirtz@cos.uni-heidelberg.de

25

26 Carmela Giglione

27 Phone: + 33-169-823597

28 E-mail: carmela.giglione@i2bc.paris-saclay.fr

29

30 **Author contributions:** MH, EL and Ist identified and characterized the NatB-depleted
31 mutants under non-stressed and osmotic stress conditions. CG and TM supervised the N-
32 terminal acetylome profiling. WVB profiled N-termini of the NatB-depleted mutants and wild-
33 type. CG, TM and WVB analyzed the N-termini data. CS performed the global transcriptome

34 analysis. DL and KL expressed, purified and analyzed the *At*NatB complex. IS supervised
35 and planned the biochemical characterization of *At*NatB. LA performed the bioinformatics
36 prediction of NatB substrates based on the substrate specificity elucidated in this paper. MW
37 and RH conceived and directed the study, MW, LA, CG and TM wrote the manuscript with
38 inputs from all authors.

39

40

41 **Funding information:** Research at Heidelberg was funded by the German Research
42 Council (DFG) via the Collaborative Research Centre 1036 (TP 13 to RH and MW, and TP
43 22 to IS), and the Leibniz Programme to I.S., and by the European Union by the ERA-CAPS
44 project KatNat to MW and CG. Research in CG lab was supported by ANR Energiome and
45 Sciences-Paris-Saclay. RH and IS are investigators of the Cluster of
46 Excellence:CellNetworks.

47

48

49 **Abstract (250 words)**

50 N-terminal acetylation (NTA) is one of the most abundant protein modifications in
51 eukaryotes. In humans, NTA is catalyzed by seven N^α-acetyltransferases (NatA–F
52 and NatH). Remarkably, the plant Nat machinery and its biological relevance remain
53 poorly understood, although NTA has gained recognition as a key regulator of crucial
54 processes such as protein turnover, protein–protein interaction, and protein targeting.
55 In this study, we combined *in vitro* assays, reverse genetics, quantitative N-
56 terminomics, transcriptomics, and physiological assays to characterize the
57 Arabidopsis NatB complex. We show that the plant NatB catalytic (NAA20) and
58 auxiliary subunit (NAA25) form a stable heterodimeric complex that accepts
59 canonical NatB-type substrates *in vitro*. *In planta*, NatB complex formation was
60 essential for enzymatic activity. Depletion of NatB subunits to 30% of the wild-type
61 level in three Arabidopsis T-DNA insertion mutants (*naa20-1*, *naa20-2*, and *naa25-1*)
62 caused a 50% decrease in plant growth. A complementation approach revealed
63 functional conservation between plant and human catalytic NatB subunits, whereas
64 yeast NAA20 failed to complement *naa20-1*. Quantitative N-terminomics of
65 approximately 1,000 peptides identified 32 *bona fide* substrates of the plant NatB
66 complex. *In vivo*, NatB was seen to preferentially acetylate N-termini starting with the
67 initiator methionine followed by acidic amino acids and contributed 20% of the
68 acetylation marks in the detected plant proteome. Global transcriptome and proteome
69 analyses of NatB-depleted mutants suggested a function of NatB in multiple stress
70 responses. Indeed, loss of NatB function, but not NatA, increased plant sensitivity
71 towards osmotic and high-salt stress, indicating that NatB is required for tolerance of
72 these abiotic stressors.

73

74

75 **Introduction**

76 N^α-terminal acetylation (NTA) is a global proteome imprinting mechanism conserved
77 in all three domains of life and affecting up to 60% of the soluble yeast proteins and
78 80–90% of the soluble proteins in *Arabidopsis thaliana* and humans (Polevoda and
79 Sherman, 2003; Falb et al., 2006; Arnesen et al., 2009a; Bienvenut et al., 2012).
80 Despite the prevalent frequency of N-terminal acetylation marks in the proteomes of
81 multi-cellular eukaryotes, the general function of NTA is still discussed
82 controversially. Whereas for individual proteins NTA has been shown to affect
83 folding, aggregation, subcellular localization, degradation, and protein-protein
84 interactions, the overall significance of NTA remains enigmatic (Aksnes et al., 2016).
85 NTA is catalyzed by N-terminal acetyltransferase (Nat) complexes consisting of at
86 least one catalytic subunit and one facultative auxiliary subunit. The auxiliary subunits
87 are in some cases required for catalytic activity and anchor the catalytic subunit to
88 the ribosome (Aksnes et al., 2015a; Aksnes et al., 2019). Since all five yeast Nat
89 complexes, NatA–E, are ribosome-associated and no deacetylases acting on the N-
90 terminus are known, NTA has long been viewed as a static co-translational
91 modification targeting mostly cytosolic proteins (Polevoda et al., 2009; Arnesen,
92 2011; Giglione et al., 2015). This dogma is challenged by the recent identification of
93 many partially acetylated proteins and post-translational NTA via the Nat complexes
94 NatF–H in multicellular eukaryotes (Linster and Wirtz, 2018; Aksnes et al., 2019).
95 In humans, the Golgi-associated NatF and the cytosolic NatH control the acetylation
96 of membrane proteins as well as cytoskeleton assembly and cell motility (Drazic et
97 al., 2018). Whereas a NatH homolog is absent in the plant lineage of eukaryotes, a
98 potential homolog of NatF is present in the *Arabidopsis* genome. The function of the
99 human and plant NatF might differ since the most relevant phenotype of NatF-
100 depleted human cells is the disruption of the Golgi-association with the nucleus
101 (Aksnes et al., 2015b), a feature that plant cells inherently lack (Dupree and Sherrier,
102 1998). NatG is a plant-specific acetyltransferase that localizes to the plastids, where
103 it acetylates N-termini of plastid-encoded as well as imported nuclear-encoded
104 proteins (Dinh et al., 2015). These differences in the post-translationally acting NTA
105 machinery of plants and humans suggest specific adaptations of the NTA in photo-
106 autotrophic eukaryotes and allows for questioning the conservation of the ribosome-
107 associated NTA machinery in eukaryotes.

108 In a recent study, we demonstrated that the drought stress-related phytohormone
109 abscisic acid (ABA) quickly depleted NatA abundance and thereby altered the
110 plasticity of N-terminal protein acetylation. Remarkably, down-regulation of NatA by
111 genetic engineering resulted in constitutive activation of the ABA response and,
112 consequently, drought-resistant plants (Linster et al., 2015). These findings suggest
113 that NTA in plants is not static but a highly dynamic process, which responds to
114 environmental cues and contributes to the regulation of stress responses. Such
115 active control of NTA has not been observed in other eukaryotes yet and might
116 constitute an adaptation to the sessile lifestyle of plants which forces them to cope
117 with a variety of biotic and abiotic perturbations (Linster and Wirtz, 2018). However,
118 the substrate specificity and the functions of the catalytically active (NAA10) and the
119 ribosome anchor subunit (NAA15) of NatA are conserved between plants and
120 humans (Linster et al., 2015).

121 NatA acetylates N-termini of nascent polypeptide chains after removal of the initiator
122 methionine (iMet) by methionine aminopeptidases (Frottin et al., 2006). By contrast,
123 NatB recognizes the iMet when it is followed by the acidic amino acids aspartate or
124 glutamate, or its amidated analogs asparagine and glutamine in yeast and human
125 (Aksnes et al., 2019). Orthologous proteins of the NatB subunits NAA20 (At1g03150)
126 and NAA25 (At5g58450) are encoded in the Arabidopsis genome (Bienvenut et al.,
127 2012; Ferrandez-Ayela et al., 2013), but the substrate specificity of this potential plant
128 NatB complex is unknown. Recently, NatB was shown to accept the plant immune
129 receptor SNC1 (Suppressor of NPR1, Constitutive 1) as a substrate, when the
130 alternative translation of the SNC1 protein usually starting with MMD generates the
131 MD-SNC1 variant. Since NatA recognizes MMD-SNC1, the SNC1 protein is
132 acetylated either by NatA or NatB, which defines SNC1 as an unusual case for
133 substrate recognition by Nat complexes. By controlling the stability of SNC1, NatB
134 contributed in the defense response to the pathogen *Hyaloperonospora arabidopsidis*
135 Noco2 (Xu et al., 2015).

136 Up to now, it was unclear if NatB is also involved in the control of plant abiotic stress
137 responses, and if the substrate specificity and the complex stoichiometry of NatB are
138 conserved in plants.

139 In this study, biochemical characterization of the potential Arabidopsis NatB subunits
140 NAA20 and NAA25 revealed that they form *in vitro* a stable heterodimeric complex,
141 which accepts canonical NatB-type substrates found in other eukaryotes. We show

142 that T-DNA insertions in the NatB mutants did not cause full inactivation but depletion
143 of NatB subunits to 30% of wild-type (WT) level. This NatB depletion caused
144 significant retardation of growth, which leads to the hypothesis that NatB is
145 indispensable in plants. N-terminal acetylome profiling of the wild-type and *At*NatB-
146 depleted mutants characterized 1,736 total N-termini including 738 unique protein
147 entries. The dataset allowed comparison of the quantification of the acetylation level
148 of 247 unique proteoforms in either genotype with the wild-type. Out of these
149 proteoforms, 70% (514) were substrates of the N-terminal methionine excision (NME)
150 process and 30% (224) did not undergo removal of the first methionine (iMet). The
151 comparison of NTA frequency in wild-type and NatB-depleted plants identified 35
152 NatB substrates which were most sensitive to depletion of NatB activity and
153 unraveled significant conservation of the NatB substrate specificity in eukaryotes.
154 Remarkably, NatB-mediated proteome imprinting is essential for adaptation to salt
155 and osmotic stress in *Arabidopsis thaliana*. The global transcriptome and proteomic
156 analyses of NatB mutants reinforce the role of *At*NatB in cellular stress responses
157 and provide a valuable resource to screen for other metabolic processes affected by
158 NatB depletion in plants.

159

160 **Results**

161 ***At*NAA20 and *At*NAA25 form a stable heterodimeric complex that acetylates** 162 **NatB-like substrates *in vitro***

163 Whereas homologs of the two NatB subunits NAA20 and NAA25 have been
164 identified in the Arabidopsis genome (Bienvenut et al., 2012; Ferrandez-Ayela et al.,
165 2013), complex formation and biochemical properties of the candidate plant NatB
166 subunits have not been addressed. To determine the stoichiometry of the *At*NatB
167 complex, *At*NAA25_{64–1065} and *At*NAA20_{1–150}His₆ were co-expressed in insect cells and
168 purified to homogeneity (Supplementary Figure 1); *At*NAA20_{1–150}His₆ is highly
169 unstable when expressed without its interaction partner *At*NAA25. Size exclusion
170 chromatography coupled to multi-angle light scattering (SEC-MALS) analysis of the
171 purified proteins revealed that in solution NAA20 and NAA25 form a stable
172 heterodimeric complex (measured $M_w = 132.1 \pm 0.9$ kDa; theoretical $M_w = 132.4$ kDa,
173 Figure 1A).

174 Although *At*NAA20 had been recognized as an N-terminal acetyltransferase (Xu et
175 al., 2015), the substrate specificity of free NAA20 and the plant NatB complex
176 remained elusive. To address this aspect, we applied both *in vitro* and *in vivo*
177 acetylation assays. For the *in vitro* assay, five peptides representing canonical
178 substrates of the major eukaryotic Nats were tested with the purified NatB complex.
179 The known *in vitro* substrates of NatA (SESS, Ree et al. (2015); Weyer et al. (2017)),
180 Naa10/Naa80 (EEEI, Casey et al. (2015); Drazic et al. (2018)), and NatC/E/F
181 (MVNALE and MLGTE, Van Damme et al. (2011)) were not acetylated. *At*NatB was,
182 however, able to acetylate the canonical substrate of human NatB (MDEL, Figure 1B,
183 Starheim et al., (2008)). Therefore, the MDEL peptide was used to determine the
184 enzymatic parameters of the plant NatB complex. The acetyltransferase shows a
185 Michaelis-Menten constant (K_m) of $38.4 \pm 9.1 \mu\text{M}$ for its substrate acetyl-Coenzyme A
186 (acetyl -CoA) and a turnover rate (k_{cat}) of $27.3 \pm 1.6 \text{ min}^{-1}$. This is in good agreement
187 with the k_{cat}/K_m value observed for *Candida albicans* NatB (Figure 3C-D, Hong et al.
188 (2017)). Noteworthy, the K_m of NatA (Liszczyk et al. (2013); Weyer et al. (2017)),
189 NatB (Hong et al. (2017); this study), and Naa50 (Liszczyk et al. (2013)) for acetyl-
190 CoA are all in the range of 24–59 μM . In comparison with other enzymes using
191 acetyl-CoA in the cytosol of plant cells (e.g., serine acetyltransferase, $K_m = 0.28 \text{ mM}$,
192 (Noji et al., 1998)), the K_m measured for *At*NatB is low, indicating sufficient affinity for
193 acetyl-CoA to trigger efficient catalysis by *At*NatB *in planta*.

194 **Downregulation of NatB activity leads to retarded growth**

195 In order to evaluate the impact of NatB depletion on plant development, we analyzed
196 the T-DNA insertion lines *naa20-1* (SALK_027687) and *naa25-1* (GK-819A05)
197 affected in the catalytic subunit (NAA20) or the auxiliary subunit (NAA25) of *At*NatB.
198 Quantification of the rosette radius over time revealed a slow growth of both mutants
199 in comparison to the wild-type (Figure 2A, B). After seven weeks, NatB mutants
200 reached approximately 75% of the wild-type size and 50% of its total rosette fresh
201 weight (Figure 2B, Supplementary Figure 2 and 3). A similar growth retardation was
202 observed in the NatB T-DNA insertion line *naa20-2* (SAIL_323_B05), which had
203 previously been characterized by Ferrandez-Ayela et al. (2013) (Supplementary
204 Figure 2E). Since Ferrández-Ayela and colleagues had reported defects in embryo
205 development of *naa20-2*, we quantified viable pollen and seeds per silique in the
206 *naa20-1* and *naa25-1* mutants. No significant differences in comparison to wild-type
207 plants were detected when plants were grown under short-day conditions and optimal

208 nutrient supply (Supplementary Figure 4). This discrepancy might be explained by
209 the different growth conditions used in both studies.

210 We quantified the impact of the T-DNA insertion in the *NAA20* and *NAA25* genes on
211 the expression of NatB subunits by analyzing the abundance of *NAA20* and *NAA25*
212 transcripts via RT-qPCR. In both, *naa20-1* and *naa25-1* lines, remaining *NAA20* or
213 *NAA25* transcripts could be detected (Figure 2C, D). In addition, the translation of the
214 *NAA25* transcript was verified with a specific antiserum, confirming that *naa25*
215 mutants retain 30% of the wild-type *NAA25* protein level (Figure 2E, F). These
216 findings demonstrate that *naa20-1* and *naa25-1* are not loss-of-function NatB
217 mutants, but were significantly depleted in NatB abundance.

218 **The human NAA20 homologue can functionally complement the Arabidopsis** 219 ***naa20* mutant**

220 To verify whether the T-DNA insertion in the *NAA20* gene was causative for the
221 *naa20-1* phenotype, the mutant was complemented with a construct expressing the
222 endogenous Arabidopsis *NAA20* protein (*AtNAA20*) under the control of the
223 constitutive CaMV 35S promoter. The successful transformation was confirmed by
224 PCR-based genotyping (Supplementary Figure 5A). The resulting complemented
225 *naa20-1* mutants had a wild-type-like habitus and a relative rosette dry weight
226 indistinguishable from the wild-type control (Figure 3A, -C). When expressed via the
227 same construct, the human *NAA20* orthologue (*HsNAA20*) was able to rescue the
228 Arabidopsis *naa20-1* phenotype as well (Figure 3A, 3C, Supplementary Figure 5B).
229 Remarkably, expression of the yeast *NAA20* protein (*ScNAA20*) using the same
230 promoter, ribosome binding site, and terminator failed to complement *naa20-1*,
231 although the *ScNAA20* transcript was produced as shown by semi-quantitative RT-
232 PCR (Figure 3B, C, Supplementary Figure 5C, -D, Supplementary Figure 6). This
233 observation is in agreement with the complementation of yeast *natB* loss-of-function
234 mutants by simultaneous expression of both human NatB subunits, but not of its
235 single subunits in the respective *naa20* or *naa25* single knockouts (Van Damme et
236 al., 2012). Our results suggest that endogenous *AtNAA25* assembles with *AtNAA20*
237 or *HsNAA20* to a functional NatB complex, whereas interaction with *ScNAA20* either
238 failed or produced a catalytically inactive complex *in planta*. Furthermore, one cannot
239 exclude that, unlike the *HsNAA20*, the *ScNAA20* might display a different specificity
240 with respect to some plant substrates. The relevance of species-specific differences

241 for complementation of plant loss-of-function mutants has already been evidenced in
242 the case of another N-terminal modifying enzyme, N-Myristoyltransferase (Pierre et
243 al., 2007).

244 **Bioinformatics screen for potential NatB substrates**

245 The functional conservation between the human and the Arabidopsis NAA20 protein
246 suggests that the substrate specificity of the NatB complex might also be evolutionary
247 conserved. Thus, we screened the Arabidopsis proteome for potential NatB targets
248 based on the database of known-classical NatB substrate specificity (ME, MD, MN,
249 and MQ). This search revealed 11,399 nuclear-encoded Arabidopsis protein variants
250 starting with a canonical plant NatB substrate N-terminus (23.6% of the total
251 proteome, Supplementary Table 1). For 4,927 potential NatB substrates, the
252 subcellular prediction was inconclusive according to TAIR10-Subcellular Predictions
253 (Kaundal et al., 2010). Out of the remaining 6,472 proteins with well-predicted
254 subcellular localizations, 1,010 proteins are supposed to be translated at the rough
255 ER due to their extracellular localization (472) or localization in the Golgi body (60) or
256 the cell membrane (478) (Reid and Nicchitta, 2015). 5,462 protein variants are
257 predominantly translated by cytoplasmic ribosomes, and stay in the cytoplasm (969;
258 17.7%), or are translocated to the nucleus (3,372; 61.7%), the mitochondria (589;
259 10.7%), or the plastids (532; 9.7%). At least these 5,462 proteins translated by
260 cytoplasmic ribosomes are prime candidates for proteome imprinting by NatB since
261 eukaryotic NatB is associated with cytoplasmic polyribosomes (Polevoda et al.,
262 2008).

263

264 **The Arabidopsis NatB complex targets the iMet of protein N-termini**

265 To verify the *in vivo* substrate specificity of AtNatB, we examined the N-terminomes
266 of cytosolic soluble proteins from the leaves of wild-type and NatB-depleted plants
267 (*naa20-1* and *naa25-1*) by the 'Stable Isotope Labelling Protein N-terminal
268 Acetylation Quantification' (SILProNAQ) method (Bienvenut et al. (2017a)).
269 Experimental data were then processed with the EnCOUNTER tool (Bienvenut et al.,
270 2017b) to provide an accurate measurement of the N-terminal acetylation pattern and
271 frequency in wild-type and NatB-depleted plants. Analysis of these three genotypes
272 together identified 1,736 N-termini corresponding to 738 non-redundant proteoforms

273 (Supplementary Table 2). The analysis of these unique proteoforms revealed that
274 514 (70%) underwent removal of iMet following the N-terminal methionine excision
275 rule (Frottin et al., 2006), whereas 224 proteoforms (30%) still displayed their iMet.
276 94% of the iMet starting N-termini had an amino acid with a large lateral chain at
277 position two (Supplementary Table 2).

278 Among all identified proteoforms we were able to quantify according to criteria
279 defined in Bienvenut et al., (2017b), 436 unique N-termini (271 in the wild-type, 360
280 in *naa20-1*, and 339 in *naa25-1* mutant backgrounds). Among the quantified N-
281 termini in these three genotypes, 333 underwent removal of iMet (76%) and 103
282 (24%) retained their iMet. In the wild-type, 87% (55/67) of the quantified N-termini
283 that retained the iMet were fully acetylated (acetylation yield >95%), whereas 13%
284 (12/67) were partially or not acetylated (Figure 4A, Table 1). The fully acetylated
285 proteins are predominantly classical NatB-substrates (N-termini featuring iMet
286 followed by Glu>Asp>>Asn, (48/55). Only two NatB-type N-termini were found in the
287 groups of partly or non-acetylated proteins (2/12). The groups of weakly or non-
288 acetylated proteins consisted mostly of iMet-Lys N-termini (7/12), together with three
289 putative NatC-type N-termini (iMet-Ile and iMet-Leu, 3/12).

290 The SILProNAQ approach revealed a 25% decrease in the overall N-acetylation level
291 in NatB-depleted plants (*naa20-1* and *naa25-1*) when compared to wild-type (Figure
292 4A). The acetylation frequency of N-termini devoid of the iMet was unaffected in
293 NatB-depleted mutants (Figure 4B), which is in agreement with the acceptance of
294 these N-termini as substrates by NatA (Linster et al., 2015). Remarkably, all N-termini
295 with decreased acetylation retained their iMet (Figure 4C). We identified 32 proteins
296 that were fully acetylated in the wild-type and displayed significantly less NTA in
297 NatB-depleted mutants (Table 2). Those proteins predominantly displayed the acidic
298 amino acids Asp and Glu and to a minor extent Asn at position two (Figure 4E and
299 Table 1). This set of *in planta*-detected NatB substrates independently confirms the
300 substrate specificity determined with the *in vitro* reconstituted plant NatB and are,
301 thus, defined as *bona fide* substrates in the subset of the proteome analyzed here
302 (Figure 1). Furthermore, three partly acetylated proteins in the wild-type showed
303 lowered acetylation in NatB-depleted plants. The N-terminus of the indole-3-butyric
304 acid response 1 protein (starting with iMet-Asp, AT4G05530.1) was 80% acetylated
305 in the wild-type but found to be not acetylated in NatB-depleted plants (NTA level:

306 <1%). The two remaining proteins (HMGB2 and HMGB3) had Lys at position two,
307 and their N-termini were less than 16% acetylated in the wild-type. In the NatB-
308 depleted mutants, the NTA levels of both proteins were decreased to 8–13%.

309 In addition to the 35 proteins that were less acetylated in NatB-depleted plants, we
310 observed eight in the wild-type fully acetylated proteoforms that could not be
311 quantified in NatB-depleted plants but were experimentally characterized without
312 NTA modification (Supplementary Table 2). This set of potential NatB proteins
313 included the salt stress-related protein AT1G13930 (see below). In accordance with
314 the *At*NatB substrate specificity determined here, these proteins also possess
315 Glu>Asp>Asn as second residues.

316 After characterization of the *in vivo* substrate specificity of plant NatB, we rechecked
317 the number of NatB substrate N-termini in the wild-type protein fraction and detected
318 499 N-terminal peptides of which 149 started with an iMet. Out of the iMet-retaining
319 peptides, 108 displayed an N-terminus starting with iMetAsp, iMetGlu, or iMetAsn
320 (Supplementary Table 3), which can be accepted by the plant NatB according to the
321 *in vitro* and *in vivo* analysis of the *At*NatB substrate specificity performed here (Figure
322 1 and Figure 4). This analysis defines 22% of the detected N-termini in the leaves of
323 the wild-type as substrates of NatB. Due to the remaining NatB activity (approx. 30%
324 of wild-type level) in the *naa20-1* or *naa25-1* mutants, not all of these substrates were
325 less acetylated in the mutants. Notably, the majority of potential NatB substrates
326 were found to be fully acetylated in the wild-type leaf under non-stressed conditions.
327 In agreement with the finding that approx. 22% of the detected N-termini from soluble
328 proteins match the substrate specificity of NatB, a significant increase of free N-
329 termini in NatB-depleted mutants was demonstrated by fluorescent labeling of free
330 protein N-termini with NBT-Cl (Figure 4D).

331 In parallel to the SILProNAQ analysis, a 2D gel approach was applied to identify
332 further NatB substrates. Total protein extracts from wild-type or *naa20-1* plants were
333 separated by 2D-gel electrophoresis according to their size and charge. If a basic
334 shift was observed for a protein species, this was attributed to the increased positive
335 charge of the protein due to loss of NTA. The 2D gel analysis yielded three
336 reproducible shifts (Figure 4F and Supplementary Figure 7). In the case of the salt
337 stress-related protein AT1G13930, we could verify that the N-terminal peptide (iMet-
338 Asn) of the acidic proteoform was acetylated in both genotypes whereas the basic

339 proteoform was unacetylated. These results demonstrate lowered NTA of
340 AT1G13930 in *naa20-1* when compared to wild type and independently confirm the
341 identification of AT1G13930 as a NatB substrate by the SILProNAQ approach. The
342 SILProNAQ approach also supports the lowered NTA of nucleoside diphosphate
343 kinase 1 (AT4G09320, Table 2), which was identified in spot 2 and spot 2* within the
344 2D gel approach (Figure 4F).

345

346 **NatB depletion results in sensitivity to high-salt and osmotic stress**

347 Based on the above results and the identification of the salt sensitivity modulator
348 AT1G13930 as a NatB substrate (Figure 4F), we analyzed the performance of NatB-
349 depleted mutants under high-salt and osmotic stress. To this end, seeds were
350 germinated on 1xMS medium supplemented with either 100 mM NaCl, 3% mannitol,
351 or no osmoticum. Both NatB-depleted mutants showed a significant reduction in
352 germination efficiency when grown on NaCl or mannitol, demonstrating that NatB is
353 essential for efficient germination under hyperosmotic or high-salt conditions (Figure
354 5A, -C). To prove that this diminished germination efficiency was exclusive to NatB
355 mutants rather than a pleiotropic side effect of impaired NTA at the ribosome, the
356 NatA-depleted lines *amiNAA10* and *amiNAA15* were subjected to the same stress.
357 Depletion of NatA activity did not influence the germination rate under hyperosmotic
358 or high-salt conditions (Figure 5B, -D), indicating a specific function of NatB-mediated
359 proteome imprinting during these stresses. To assess the effect of osmotic stress on
360 adult plants, wild-type and *naa20-1* mutants were grown on ½ x MS medium
361 supplemented with 1% sucrose for two-weeks under short-day conditions.
362 Subsequently, the plants were transferred to the same medium (control) or medium
363 supplemented with 150 mM NaCl. After two weeks, the growth of the primary root
364 was evaluated. Although both plants experienced salt stress as indicated by the
365 increased transcription of the salt stress marker gene *HB-7*, only *naa20-1* mutants
366 displayed a significantly impaired primary root growth on high-salt medium
367 (Supplementary Figure 8).

368 **Global transcriptome analysis of NatB-depleted mutants**

369 Based on the vast number of predicted NatB substrates, NatB depletion was
370 expected to affect a variety of cellular processes. A global analysis of the leaf
371 transcriptome revealed differential regulation (>1.5-fold up- or downregulated) of 494

372 transcripts (~2% of all tested transcripts) when comparing six-week-old soil grown
373 *naa20-1* mutants to wild-type plants (Gene Expression Omnibus record:
374 GSE132978). In this context, 322 transcripts were downregulated and 172 transcripts
375 upregulated (Supplementary Table 4). To identify putatively NatB-affected biological
376 processes, we performed a gene ontology enrichment analysis for differentially
377 regulated genes in *naa20-1* using the DAVID Bioinformatic Resources tool v. 6.8
378 (Table 3, Supplementary Table 5). Among the upregulated transcripts, genes
379 involved in transition metal transport, namely zinc ion transport, and lipid localization
380 were significantly (3-fold enrichment, $p < 0.05$) enriched. Among the downregulated
381 transcripts, however, genes mediating plant stress responses were considerably
382 overrepresented. The downregulated responses to environmental perturbations
383 included not only the reaction to light intensity or toxins but also distinct steps within
384 the immune response, e.g., responses to bacteria, fungi, viruses, wounding, and
385 reactive oxygen species. Taken together, this pattern of transcriptional regulation in
386 NatB-depleted mutants suggest an even broader function of NatB in the plant
387 immune response than previously shown by Xu et al. (2015).

388 **Discussion**

389 The Arabidopsis NatB complex is involved in a variety of developmental processes,
390 including leaf shape formation and transition from vegetative to generative growth.
391 The developmental defects observed in NatB mutants had previously been attributed
392 to a total loss-of-NatB activity (Ferrandez-Ayela et al., 2013). Here, we demonstrate
393 that the available NatB T-DNA insertion lines retain a diminished NatB expression
394 and hence do not constitute full knockouts. This finding demonstrates the importance
395 of functional NatB-mediated imprinting of the proteome with acetylation marks and
396 also raises the question towards the severity of total NatB loss-of-function. Since full
397 loss-of-function NatB mutants by T-DNA insertion are currently unavailable, this
398 question should be addressed by CRISP-Cas9 mediated gene-disruption in future
399 studies. Loss of NatA causes abortion of the plant embryo at the globular stage
400 (Linster et al., 2015). It is tempting to speculate that loss of NatB might as well be
401 lethal in plants. Remarkably, depletion of NatB activity in human cells impairs cellular
402 proliferation and affects tumorigenesis (Ametzazurra et al., 2008; Starheim et al.,
403 2008; Ametzazurra et al., 2009). In yeast, NatB is dispensable like the loss of any
404 other Nat complex. The yeast *natB* mutants showed the most severe phenotypes

405 when compared to *natA*, *natC*, *natD*, or *natE* mutants. These phenotypes included
406 cytoskeleton defects, cell cycle arrest, and severe growth retardation (Polevoda et
407 al., 2003; Singer and Shaw, 2003).

408 **NatB substrate specificity is conserved in yeast, humans, and plants**

409 Except for the NatA complex, the substrate specificity of plant Nats was barely
410 investigated in previous works (Pesaresi et al., 2003; Linster et al., 2015). This lack of
411 knowledge prompted us to determine the NatB substrate specificity by N-terminal
412 acetylome profiling of NatB-depleted mutants and by analyzing the enzymatic activity
413 of reconstituted *At*NatB *in vitro*. Biochemical characterization of the heterodimeric
414 plant NatB and the proteomic approach revealed a clear preference of NatB towards
415 N-termini retaining their iMet followed by glutamate or aspartate. To a minor extent,
416 iMet followed by asparagine were also accepted as substrate in the subset of the leaf
417 proteome analyzed here. The recognition of those substrates recapitulates the
418 established substrate specificity of yeast and human NatB (Helbig et al., 2010; Van
419 Damme et al., 2012) and suggests significant conservation of NatB substrate
420 specificity in fungi, animals, and plants. Despite the conserved substrate specificity of
421 eukaryotic NatB complexes, only *Hs*NAA20 but not *Sc*NAA20 was able to
422 complement the retarded growth phenotype of *naa20-1* plants. A similar observation
423 was reported for NatA, whereby yeast loss-of-function NatA mutants are rescued by
424 reconstituted human NatA complex, whereas the human catalytic or auxiliary NatA
425 subunits alone cannot complement the respective single loss-of-function mutants,
426 suggesting significant structural subunit differences between the species (Arnesen et
427 al., 2009b). Similarly, significant differences in the complex assembly have been
428 reported for *At*NatC and *Sc*NatC (Pesaresi et al., 2003).

429 The substrate specificity of plant NatB determined here suggests that ~24% of the
430 plant proteome is imprinted by NatB (bioinformatical prediction). In agreement with
431 such a high number of NatB substrates, 21% of the proteins whose N-terminus could
432 be quantified in wild-type and NatB mutants were identified as substrates of NatB.
433 Such broad substrate recognition has also been determined for NatB of other
434 eukaryotes (Helbig et al., 2010; Van Damme et al., 2012), and can be explained by
435 the predominant interaction of the first two amino acids of the substrate peptide with
436 the active site of the catalytic NatB subunit (Hong et al., 2017). Furthermore,
437 depletion of *At*NatB to 30% of wild-type level in *naa20-1* and *naa25-1* caused more

438 than an 1.5-fold increase of total free N-termini (Figure 4). Since the NatB-depleted
439 mutants retain 30% of the wild-type NatB activity, we could only identify 35 substrates
440 to be unambiguously less acetylated in *naa20-1* and *naa25-1* mutants. Thus, these
441 35 proteins represent the apparently most sensitive substrates of AtNatB in leaves.

442 The proteins encoded by AT5G10780 and AT1G64520 carry the amino acid
443 aspartate as penultimate residue and are both 99% acetylated in wild-type plants.
444 Remarkably, the knockdown of NatB in *naa20* or *naa25* mutants reduced the
445 acetylation yield for AT1G64520 to 2%, whereas the protein encoded by AT5G10780
446 remained acetylated to 87–88% in the mutant. Thus, the substrate specificity and
447 degree of acetylation by NatB predominantly depends on the first two amino acids
448 but is also shaped by additional primary sequence information or the secondary
449 structure of the nascent chain. In this respect, a recent study demonstrated that
450 alpha-helices could fold co-translationally within the ribosomal exit tunnel (Nilsson et
451 al., 2015), which may interfere with binding into the catalytic pocket of NAA20.

452

453 **Acetylation via different Nats regulates specific plant stress responses**

454 Unlike NatA, which had previously been shown to mediate the drought stress
455 response in *Arabidopsis thaliana*, NatB has not previously been associated with any
456 plant abiotic stress response. The vast number of potential NatB substrates and the
457 overall decrease of stress-responses at the transcriptional level in *naa20-1* mutants
458 prompted us to analyze the performance of NatB-depleted mutants upon protein-
459 harming stress. We selected high-salt and osmotic stress because both cause
460 misfolding of proteins and consequently affects proteostasis (Chen et al., 2019).
461 Indeed, plant NatB mutants were sensitive to osmotic stress, which has also been
462 shown for yeast NatB mutants (Van Damme et al., 2012). A protective role of
463 ScNAA20-dependent acetylation with respect to protein degradation and
464 susceptibility to specific stresses has been suggested (Nguyen et al., 2019). Notably,
465 the depletion of NatA activity did not lead to hypersensitivity against osmotic or high-
466 salt stress in plants, although NatA targets approximately twice as many substrates
467 as NatB (Linster and Wirtz, 2018). Vice versa, the knockdown of NatA results in
468 drought-tolerant plants, whereas NatB-depleted plants were drought sensitive
469 comparable to the wild-type (Linster et al., 2015). Despite the high number of

470 substrates acetylated by each Nat complex, our results support discrete functions of
471 Nat complexes in response to specific stresses.

472 In human and yeast, proteomics and transcriptome analysis of NatB-depleted cells
473 show that NatB substrates are mainly involved in DNA processing and cell cycle
474 progression (Caesar and Blomberg, 2004; Caesar et al., 2006; Ametzazurra et al.,
475 2008). The global transcriptome analysis of *naa20* mutants relates NatB-mediated
476 acetylation in plants to transition metal transport, lipid localization, and stress
477 responses. One particular stress response of interest is defense against pathogens.
478 Among the transcripts downregulated in *naa20* mutants, transcripts implicated in the
479 defense against pathogens are significantly enriched, which might translate into a
480 weaker response to biotic stresses in NatB-depleted plants. Indeed, a connection
481 between Nat-mediated protein stability and pathogen resistance was recently shown
482 by Xu et al. (2015). Xu and colleagues found that a depletion of NatB subunits in
483 *Arabidopsis* caused decreased immunity against the virulent oomycete
484 *Hyaloperonospora arabidopsidis* Noco2 mediated by destabilization of the plant
485 immune receptor SNC1 (Suppressor of NPR1, Constitutive 1). Interestingly, the
486 stability of SNC1 is antagonistically regulated by NatB and NatA. Whereas
487 acetylation of the receptor via NatA serves as a degradation signal, acetylation via
488 NatB stabilizes SNC1 (Xu et al., 2015).

489 **Conclusion**

490 NTA by the NatB complex has been well characterized in yeast and humans;
491 however, the role of NatB in phototrophic organisms was less clear. The combination
492 of biochemical and reverse genetic approaches presented here elucidate the
493 substrate specificity and stoichiometry of subunits in the *Arabidopsis* NatB complex
494 and reveal the global transcriptional consequences of NatB downregulation. The
495 high-salt and osmotic stress experiments performed here uncover a specific role of
496 the *At*NatB complex under physiologically relevant abiotic stresses. These findings
497 expand the view on NatB function beyond its influence on plant development. In
498 combination with our previous findings on the role of NatA in the plant drought stress
499 response, these results encourage speculation that dynamic regulation of N-terminal
500 protein acetylation modulates plant stress responses and that distinct Nat complexes
501 have specific roles in this modulation.

502 **Materials and Methods**

503 **Plant material and growth conditions**

504 All work was performed with *Arabidopsis thaliana* ecotype Columbia-0 (Col-0). The
505 utilized T-DNA insertion lines *naa20-1* (SALK_027687, successfully selected on
506 kanamycin), *naa20-2* (SAIL_323_B05, successfully selected on glufosinate), and
507 *naa25-1* (GK-819A05, not selected on sulfadiazine in this study) originate from the
508 SALK, SAIL, and GABI-KAT collections (Sessions et al., 2002; Alonso et al., 2003;
509 Rosso et al., 2003), respectively. The NatA artificial microRNA (amiRNA) knock-down
510 lines *amiNAA10* and *amiNAA15* were created by Linster et al. (2015). All experiments
511 except the osmotic stress treatment (described below) were conducted with plants
512 grown on medium containing one half soil and one half substrate 2 (Klasmann-
513 Deilmann, Germany) under short-day conditions (8.5-h light, 100 μ E light photon flux
514 density, 24°C/18°C day/night temperatures, and 50% humidity).

515 **Osmotic stress treatment**

516 To analyze the implications of NatB-mediated N-terminal acetylation under osmotic
517 stress, seeds of NatB-depleted mutants were surface-sterilized with 70% (v/v)
518 ethanol (5 min) and 6% (v/v) NaClO (2 min) followed by three washing steps with
519 sterile water. After two days of stratification at 4°C, seeds were germinated under
520 short-day conditions on 1x Murashige & Skoog (MS) medium (4 g/l MS-salts
521 (Duchefa, Netherlands), 1% (w/v) sucrose, 0.4 g/l MES, 0.7% (w/v) micro agar, pH
522 5.9). To induce osmotic stress, plates were supplemented with either 100 mM NaCl
523 or 3% (w/v) mannitol.

524 To assess the effect of osmotic stress on adult plants, seeds of wild-type and *naa20-1*
525 mutants were surface sterilized and stratified as described above. The plants were
526 grown on ½ x MS medium supplemented with 1% (w/v) sucrose for two weeks under
527 short-day conditions. Subsequently, the plants were transferred to the same medium
528 (control) or medium supplemented with 150 mM NaCl. After two weeks, the growth of
529 the primary root was evaluated. The transcript levels of the salt stress marker *HB-7*
530 (AT2G46680, Liu et al., 2007) and the putative NatB substrate salt stress-related
531 protein (AT1G13930) were assessed via reverse transcription quantitative PCR (RT-
532 qPCR; see below).

533 **PCR**

534 PCR for identification of T-DNA insertion lines was performed with the Taq-DNA
535 Polymerase (New England Biolabs, M0267L). Genotyping of T-DNA insertion lines

536 *naa20-1*, *naa20-2*, and *naa25* was conducted with specific primer combinations for
537 the wild-type (NAA20_LP, NAA20_RP, NAA25_LP, and NAA25_RP) and mutant
538 allele (SALK_BP and GK_BP). For cloning, DNA was amplified with the high-fidelity
539 DNA polymerase Phusion (New England Biolabs, M0530L). All enzymes were used
540 according to the supplier's instructions manual. The corresponding primer sequences
541 are listed in the Supplementary Table 6.

542 **Reverse transcription quantitative PCR**

543 To analyze Nat transcript levels, total RNA was extracted from leaves using the
544 RNeasy Plant Kit (Qiagen, Germany). Subsequently, total RNA was transcribed into
545 complementary DNA (cDNA) with the RevertAid H Minus First Strand cDNA
546 Synthesis Kit using oligo(dT) primers (Thermo Scientific). All reactions were
547 conducted according to the supplier's protocol. The cDNA was analyzed by qPCR
548 with the qPCRBIO SyGreen Mix Lo-ROX (PCR Biosystems) and TIP41 (AT4G34270,
549 Czechowski et al. (2005)) as reference gene. The primer sequences for specific
550 amplification of genes are listed in the Supplementary Table 6. Data was analyzed
551 via Rotor-Gene Q Series Software (v2.0.2).

552 **Stable transformation of *Arabidopsis thaliana***

553 To analyze the conservation between NAA20 orthologues, the *Arabidopsis naa20-1*
554 line was transformed with the endogenous NAA20 sequence as well as the human
555 and yeast NAA20 sequences. The genes of interest were amplified via PCR using
556 Gateway compatible primers (*At*NAA20-N, *At*NAA20-C, *Hs*NAA20-N, *Hs*NAA20-C,
557 *Sc*NAA20-N, and *Sc*NAA20-C, see Supplementary table 6). The NAA20 sequences
558 were then cloned into the binary vector pB2GW7, where they were expressed under
559 the control of the CaMV 35S promoter. Stable transformation was conducted
560 according to the floral dip method for *Agrobacterium*-mediated transformation of
561 *Arabidopsis thaliana* described by Clough and Bent (1998). Transformants were
562 selected using 200 mg/l BASTA at the age of two weeks. The presence of stably
563 transformed constructs was confirmed using primers either amplifying the BASTA
564 (BASTA_fw and BASTA_rev) or the *Sc*NAA20 (*Sc*Nat3_fw and *Sc*Nat3_rev)
565 sequence. To control the expression of the *Sc*NAA20 construct, semi-quantitative
566 RT-PCR was performed via Taq-DNA Polymerase using the housekeeping gene
567 actin as a positive control (*Sc*NAA20_fwd, *Sc*NAA20_rev, Actin_fwd, and Actin_rev).

568 **Generation of a NAA25-specific antibody**

569 The DNA sequence encoding the amino acids 233–430 of NAA25 was PCR amplified
570 with primers comprising restriction sites for NcoI and HindIII (NAA25_fwd and
571 NAA25_rev, Supplementary Table 6) and cloned into pET20b (C-terminal His-fusion)
572 using the newly introduced restriction sites. Correct cloning was verified by DNA
573 sequencing. For protein expression, the vector was transformed into *E. coli Rosetta*
574 *DE3 pLysS* (Novagen) by electroporation. Cell cultures were grown in 300 ml
575 selective LB medium at 37°C and protein expression was induced at an OD₆₀₀ of 0.8
576 with 1 mM IPTG (isopropyl-β-D-thiogalactoside). After 5 h of incubation, the cells
577 were harvested by centrifugation and stored at -80°C until further usage. *E. coli*
578 pellets containing recombinant proteins were lysed by sonication in 5 ml
579 resuspension buffer (250 mM NaCl, 50 mM Tris pH 8.0 supplemented with 0.5 mM
580 PMSF). The crude extract was centrifuged and the resulting pellet was dissolved in
581 10 ml denaturation buffer (8 M urea, 10 mM NaH₂PO₄, 1 mM Tris, pH 8.0) using the
582 Ultra-Turrax® T25. The protein fraction was cleared by centrifugation (10 min at
583 26,400 g, 4°C). The supernatant was used for further separation via SDS-PAGE. The
584 NAA25 fragment band was cut out and the protein was eluted in denaturation buffer
585 using the electro elution chamber Biotrap BT 1000 (Schleicher and Schuell)
586 according the manufacturer's instructions. The denatured protein fraction was
587 concentrated using the Vivaspin® 2 Centrifugal Concentrator (10.000 MWCO PES)
588 and used for the immunization of rabbits.

589 **Protein extraction from Arabidopsis leaf tissue**

590 Total soluble protein extracts were isolated from 200 mg ground leaf material using
591 500 µl pre-cooled extraction buffer (50 mM HEPES pH 7.4, 10 mM KCl, 1 mM EDTA,
592 1 mM EGTA, 10% v/v glycerol) supplemented with 10 mM DTT and 0.5 mM PMSF.
593 Protein extracts were cleared by centrifugation (10 min at 20,200 g, 4°C) and the
594 protein concentration was quantified according to Bradford (1976).

595 **SDS-PAGE and immunological detection**

596 Protein extracts were subjected to SDS-PAGE according to Laemmli (1970) and
597 blotted to a PVDF membrane using Mini-Protean™ II cells (BioRad). The primary
598 NAA25 antibody and the secondary horseradish peroxidase-linked anti-rabbit
599 antibody (#AS10 852, Agrisera) were diluted 1:5,000 and 1:25,000 in 1x TBS-T
600 (50 mM Tris pH 7.6, 150 mM NaCl, 0.05% (v/v) Tween-20) supplemented with 0.5%

601 (w/v) BSA. Membranes were developed using the SuperSignal West Dura Extended
602 Duration Substrate (Thermo Scientific) according to the manufacturer's instructions.
603 The resulting signals were recorded using the ImageQuant LAS 4,000 (GE
604 Healthcare) and subsequently quantified with the ImageQuant TL Software (GE
605 Healthcare).

606 **Separation of total Arabidopsis protein by two-dimensional PAGE**

607 To identify putative NatB substrates, 200 mg leaf material of nine-week-old, soil-
608 grown wild-type and *naa20* plants was ground in liquid nitrogen. Proteins were
609 precipitated with trichloric acid/acetone. Subsequently, 160 mg protein of protein
610 were subjected to isoelectric focusing followed by SDS-PAGE as described in Heeg et
611 al., 2008. The separated proteins were visualized by silver staining (Blum et al.,
612 1987). Putative substrates were identified with MALDI-TOF-MS analysis as outlined
613 in Heeg et al., 2008.

614 **Determination of the global transcriptome**

615 The peqGOLD Total RNA Kit (Pepqlab) was used to extract RNA from 17-day-old wild-
616 type and *naa20-1* seedlings grown on 1xMS medium under short-day conditions. A
617 global transcriptome analysis was performed using the Affimetrix (High Wycombe,
618 UK) *Arabidopsis thaliana* Genechip (AraGene-1_0st-typ) as described in detail by
619 Linster et al., 2015. Transcripts which were differentially regulated (>1.5-fold up- or
620 downregulated, $p < 0.05$) in *naa20-1* compared to wild-type were functionally
621 annotated. Overrepresented biological processes were identified based on the
622 DAVID Bioinformatics Resources 6.8 gene ontology analysis (Huang da et al., 2009b,
623 a).

624 **Quantification of N-terminal protein acetylation**

625 Soluble leaf proteins from six-week-old soil-grown wild-type and the NatB-depleted
626 mutants, *naa20-1* and *naa25-1*, were extracted for quantification of N-terminal protein
627 acetylation. The extracted proteins were processed and enriched by an SCX
628 approach for quantification of N-terminal peptides using mass spectrometry as
629 described in Linster et al., (2015).

630 **Determination of free N-termini**

631 To determine the relative amount of free N-termini in wild-type, *naa20-1*, and *naa25-1*
632 plants, soluble proteins were extracted from leaf material (50 mM sodium citrate
633 buffer pH 7.0, 1 mM EDTA). For removal of free amino acids, protein extracts were
634 subsequently gel filtrated via PDMiniTrap G-25 columns (GE Healthcare). The
635 labeling of free N-termini was performed with 2.5 μ M extracted protein and 0.5 mM
636 NBD-Cl (Bernal-Perez et al., 2012) in 50 mM sodium citrate buffer pH 7.0
637 supplemented with 1 mM EDTA. After 14 h of incubation at room temperature, the
638 fluorescence intensity was quantified via a FLUOstar Omega plate reader (BMG
639 Labtech; excitation: 470 \pm 10; emission: 520 nm).

640 **Construction of AtNatB Baculovirus**

641 *AtNAA25*_{64–1065} and *AtNAA20*_{1–150} coding sequences were amplified by PCR from
642 *Arabidopsis thaliana* cDNA and a C-terminal His-tag was introduced into the
643 *AtNAA20* sequence (Supplementary Table 1). The PCR products were cloned into
644 pET24d and pET21d (Novagen), respectively. *AtNAA25*_{64–1065} and *AtNAA20*_{1–150}His₆
645 coding sequences were subcloned from the pET vectors into a pFastBacDUAL vector
646 (Invitrogen). A bacmid was generated by transferring the plasmid into
647 electrocompetent DH10 MultiBac *E. coli* cells (Geneva Biotech). Afterwards, the
648 Escort IV Transfection reactant (Sigma) was used to transfect *Spodoptera frugiperda*
649 (Sf9) cells, cultured in SFM II medium supplemented with 5% (v/v) EX-CELL
650 TiterHigh (Sigma) and appropriate antibiotics, with the obtained bacmid DNA. Finally,
651 the baculovirus was amplified twice before using it for protein expression.

652 **Protein purification**

653 Sf9 insect cells were grown in SFM II medium supplemented with 5% (v/v) EX-CELL
654 TiterHigh (Sigma) and appropriate antibiotics to a density of 8x10⁵ cells/ml. 250 ml of
655 cultures were infected using the *AtNAA25*_{64–1065} *AtNAA20*_{1–150}His₆ baculovirus. The
656 cells were grown at 27 °C and harvested after 3 days by centrifugation (15 min, 1,500
657 g at 4°C). For purification, the harvested cells were resuspended in lysis buffer
658 (20 mM HEPES pH 7.5, 500 mM NaCl, 20 mM MgCl₂, 20 mM KCl, 20 mM Imidazole,
659 supplemented with protease inhibitor mix and benzonase) and lysed using a
660 microfluidizer (M-110L, Microfluidics). The lysate was cleared by ultra-centrifugation
661 (50,000 g, 30 min, 4°C) and the supernatant was loaded on Ni-NTA beads (Qiagen).

662 The *At*NAA25_{64–1065} *At*NAA20_{1–150}His₆ complex was eluted using lysis buffer
663 supplemented with 250 mM imidazole and loaded on a Superdex 200 16/60 gel-
664 filtration column (GE Healthcare) equilibrated in gel-filtration buffer (20 mM HEPES
665 pH 7.5, 500 mM NaCl) for size exclusion chromatography.

666 **Multi-angle light scattering (MALS)**

667 0.1 mg *At*NAA25_{64–1065} *At*NAA20_{1–150}His₆ was injected onto a Superdex 200 10/300
668 gel-filtration column (GE Healthcare) in gel-filtration buffer. The column was
669 connected to a MALS system (Dawn Heleos II 8+ and Optilab T-rEX, Wyatt
670 Technology). Measurements were performed in triplicates and data was analyzed
671 using the Astra 6 software (Wyatt Technology).

672 ***In vitro* acetyltransferase assays**

673 Acetylation activity of *At*NAA25_{64–1065} *At*NAA20_{1–50}His₆ was recorded using a
674 SpectraMax M5e MultiMode Microplate reader by continuously detecting the
675 absorbance at 412 nm. The assays were performed at 25°C with 1.0 mM MDEL
676 peptide (PLS GmbH) mixed with Acetyl CoA (12.5–500 μM) in reaction buffer (2 mM
677 5,5'-dithiobis(2-nitrobenzoic acid), 70 mM HEPES pH 7.5, 70 mM NaCl, 20 mM
678 sodium phosphate dibasic pH 6.8, 2 mM EDTA). The enzyme (final concentration
679 500 nM) was added to start the reaction. To determine the substrate specificity of
680 *At*NatB, various peptides (SESS, EEEI, MDEL, MVNALE, and MLGTE (all PLS
681 GmbH) and a constant AcCoA concentration of 100 μM were used. The
682 concentration of the produced CoA was quantified after 30 min. Control reactions
683 were performed in the absence of the peptides. Measurements were taken in
684 triplicates.

685 **Basic statistical analysis**

686 Statistical analysis was conducted using SigmaPlot 12.0. Means from different sets of
687 data were analyzed for statistically significant differences with the Holm-Sidak One-
688 Way ANOVA test or the student's t-test. Significant differences (P<0.05) are indicated
689 with different letters.

690 **Accession numbers**

691 Sequence data from this article can be found in the GenBank/EMBL data libraries
692 under accession numbers AtNAA20 ([LR699745.2](#)), AtNAA25 ([CP002688.1](#)),
693 AtNAA10 (CP002688.1), AtNAA15 (CP002684.1)

694

695 **Supplemental Data**

696 **Supplemental Figure S1.** Size-exclusion chromatography profile of purified AtNatB.

697 **Supplemental Figure S2.** Characterization of different *naa20* T-DNA insertion
698 mutants.

699 **Supplemental Figure S3.** Rosette fresh weight of NatB-depleted plants.

700 **Supplemental Figure S4.** Embryo development in NatB-depleted plants.

701 **Supplemental Figure S5.** Confirmation of *naa20-1* transformation and *ScNAA20*
702 expression.

703 **Supplemental Figure S6.** The Arabidopsis *naa20-1* mutant cannot be
704 complemented with the *ScNAA20* orthologue.

705 **Supplemental Figure S7.** 2D-PAGE gels comparing soluble protein extracts of nine-
706 week-old wild-type and *naa20-1* plants.

707 **Supplemental Figure S8.** Four-week-old NatB mutants are sensitive to salt stress.

708 **Supplemental Table S1.** The nuclear-encoded Arabidopsis proteome was
709 screened for potential NatB targets based on the classical NatB substrate
710 specificity (N-termini starting with ME, MD, MN or MQ).

711 **Supplemental Table S2.** Processed Data of SILProNAQ approach.

712 **Supplemental Table S3.** 108 NatB-like substrates were identified in wild-type
713 leaves.

714 **Supplemental Table S4.** Misregulated (>1.5-fold up- or downregulated, $p > 0.05$)
715 transcripts in *naa20-1* mutants compared to six-week-old soil grown wildtype
716 plants.

717 **Supplemental Table S5.** GO term enrichment analysis for differentially
718 regulated genes in NatB-depleted plants.

719 **Supplemental Table S6.** Supplemental Table S6: Primers used for genotyping,
720 RT-qPCR and amplification of *NAA20* and *NAA25*.

721

722 **Tables**

723

724 **Table 1: List of all protein N-termini without methionine excision identified and**
 725 **quantified in wild-type.** Full acetylation is defined as an N-terminal acetylation rate
 726 higher than 90%, whereas no acetylation refers to an acetylation rate lower than
 727 10%. Partially acetylated proteins range between these values.

Entry	Description	N-terminus	% NTA wild- type
AT5G10780.1	ER membrane protein complex subunit-like protein	MDKKGKAVMGT	100
AT1G06210.1	ENTH/VHS/GAT family protein	MDKCLKIAEWG	100
AT1G18070.1	Translation elongation factor EF1A/initiation factor IF2g family protein	MDLEAEIRAL	100
AT3G12800.1	short-chain dehydrogenase-reductase B	MDSPFKPDVV	100
AT2G13360.1	alanine:glyoxylate aminotransferase	MDYMYGPGRH	100
AT2G23120.1	Late embryogenesis abundant protein, group 6	MEAGKTPPTT	100
AT2G21620.1	Adenine nucleotide alpha hydrolases-like superfamily protein	MEALPEDEEY	100
AT4G13780.1	methionine-tRNA ligase, putative methionyl-tRNA synthetase, MetRS	MEDDGKSSPK	100
AT4G03560.1	two-pore channel 1	MEDPLIGRDS	100
AT2G19080.1	metaxin-like protein	MEGDQETNVY	100
AT4G24510.1	HXXXD-type acyl-transferase family protein	MEGSPVTSVR	100
AT4G15630.1	Uncharacterized protein family (UPF0497)	MEHESKNKVD	100
AT4G10060.1	Beta-glucosidase, GBA2 type family protein	MEKNGHTESE	100
AT3G45780.1	phototropin 1	MEPTEKPSTK	100
AT5G05170.1	Cellulose synthase family protein	MESEGETAGK	100
AT4G20780.1	calmodulin like 42	MESNNNEKKK	100
AT5G27670.1	histone H2A 7	MESSQATTKP	100
AT5G04430.1	binding to TOMV RNA 1L (long form)	MESTESYAAG	100
AT2G42810.1	protein phosphatase 5.2	METKNENSDV	100
AT3G04600.1	Nucleotidyl transferase superfamily protein	MEVDKKDERE	100
AT3G16250.1	NDH-dependent cyclic electron flow 1	MGSVQLSGSG	100
AT3G05870.1	anaphase-promoting complex/cyclosome 11	MKVKILRILL	100
AT3G51490.1	tonoplast monosaccharide transporter3	MRSVVLVALA	100
AT5G44316.1	ABC transporter ABCI.9	MASLFAIGFS	99.9
AT4G36250.1	aldehyde dehydrogenase 3F1	MEAMKETVEE	99.9

AT3G27890.1	NADPH:quinone oxidoreductase	MEAVTAIKPL	99.9
AT1G70810.1	Calcium-dependent lipid-binding (CaLB domain) family protein	MEELVGLLRI	99.9
AT4G09320.1	nucleoside diphosphate kinase	MEQTFIMIKP	99.9
AT5G59870.1	histone H2A 6	MESTGKVKKA	99.9
AT3G27080.1	translocase of outer membrane 20 kDa subunit 3	MDTETEFDR	99.8
AT4G34490.1	Adenylyl cyclase-associated protein	MEEDLIKRL	99.8
AT4G23710.1	vacuolar ATP synthase subunit G2	MESAGIQQLL	99.8
AT5G03660.1	transcriptional activator (DUF662)	MQPTETSQPA	99.8
AT5G03430.1	phosphoadenosine phosphosulfate (PAPS) reductase family protein	MEIDKAIGES	99.7
AT5G27640.1	translation initiation factor 3B1	MEVVDIDARA	99.7
AT4G23400.1	plasma membrane intrinsic protein 1;5	MEGKEEDVNV	99.6
AT5G54310.1	ARF-GAP domain	MNEKANVSKE	99.6
AT2G43940.1	S-adenosyl-L-methionine-dependent methyltransferases superfamily protein	MENAGKATSL	99.5
AT1G13930.1	oleosin-B3-like protein	MNFISDQVKK	99.5
AT5G54430.1	Adenine nucleotide alpha hydrolases-like superfamily protein	MNPADSDHPQ	99.5
AT4G33090.1	aminopeptidase M1	MDQFKGEPRL	99.4
AT3G48990.1	AMP-dependent synthetase and ligase family protein	MDSDTLSGLL	99.4
AT4G23730.1	Galactose mutarotase-like superfamily protein	MEPSSGTGPE	99.4
AT4G11150.1	vacuolar ATP synthase subunit E1	MNDGDVSRQI	99.4
AT3G42790.1	alfin-like 3	MEGGAALYNP	99.3
AT2G34160.1	Alba DNA/RNA-binding protein	MEEITDGVNN	99.2
AT1G02090.1	COP9 signalosome complex subunit 7	MDIEQKQAEI	99
AT1G62380.1	ACC oxidase 2	MEKNMKFPVV	98.7
AT4G24800.1	MA3 domain-containing protein1	MEGFLTDQQR	98.5
AT1G04350.1	2-oxoglutarate (2OG) and Fe(II)-dependent oxygenase superfamily protein	METKEFDSYS	98.5
AT5G19140.1	aluminum induced protein with YGL and LRDR motifs	MLGIFSGAIV	98.5
AT3G53890.1	Ribosomal protein S21e	MENDAGQVTE	98.2
AT5G43830.1	aluminum induced protein with YGL and LRDR motifs	MLAVFEKTVA	96.7
AT1G29250.1	Alba DNA/RNA-binding protein	MEEITEGVNN	96.3
AT5G16100.1	Uncharacterized protein	MAGDDPKSSA	95.9
AT4G05530.1	indole-3-butyric acid response 1	MEKKLPRRLE	82.2
AT1G05010.1	ethylene-forming enzyme	MESFPIINLE	78.9
AT5G25540.1	TC-interacting domain 6	MKSGSSTLNP	75.1
AT1G20696.1	high mobility group B3	MKGAKSKAET	15.9
AT1G20693.1	high mobility group B2	MKGAKSKTET	12
AT2G17560.1	high mobility group B4	MKGGESKAEA	6.6
AT3G59970.1	methylenetetrahydrofolate reductase MTHFR1	MKVVDKIKSV	2.9
AT4G21580.1	oxidoreductase, zinc-binding dehydrogenase family protein	MKAIVISEPG	2.6

AT5G27470.1	seryl-tRNA synthetase / serine-tRNA ligase	MLDINLFREE	2.3
AT3G07230.1	wound-responsive protein-like protein	MIYDVNSGLF	1.1
AT5G52650.1	RNA binding Plectin/S10 domain- containing protein	MIISEANRKE	0.6
AT3G55360.1	3-oxo-5-alpha-steroid 4- dehydrogenase family protein	MKVTVVSRSG	0.6

728

729

730

731

732

733 **Table 2: List of proteins found to be less acetylated in NatB-depleted plants.**
 734 Detected iMet retaining N-termini with lowered NTA in NatB mutants (*naa20-1*,
 735 *naa25-1*) compared to wild-type.

Entry	Description	N-terminus	% NTA wild- type	% NTA <i>naa20-1</i>	% NTA <i>naa25-1</i>
1	AT2G13360.1 Alanine:glyoxylate aminotransferase	MDYMYGPG	100	29.9	29.4
2	AT2G42810.1 Protein phosphatase 5.2	METKNENS	100	59.5	61.6
3	AT3G04600.1 Nucleotidyl transferase superfamily protein	MEVDKKDE	100	24	14.8
4	AT3G12800.1 Short-chain dehydrogenase-reductase B	MDSPFKPD	100	35.6	22.8
5	AT3G45780.1 Phototropin 1	MEPTEKPS	100	77.5	75.6
6	AT4G13780.1 Methionyl-tRNA synthetase	MEDDGKSS	100	n/a	8.3
7	AT4G20780.1 Calmodulin like 42	MESNNNEK	100	90.1	83.8
8	AT4G24510.1 HXXXD-type acyl-transferase family protein	MEGSPVTS	100	32.5	n/a
9	AT5G04430.1 Binds to ToMV genomic RNA and prevents viral multiplication.	MESTESYA	100	n/a	64.7
10	AT5G05170.1 Cellulose synthase isomer	MESEGETA	100	47.7	n/a
11	AT5G27670.1 Translation initiation factor 3B1	MESSQATT	100	26.5	23.2
12	AT3G27890.1 NADPH:quinone oxidoreductase	MEAVTAIK	99.9	57.8	62.5
13	AT4G09320.1 Nucleoside diphosphate kinase type 1	MEQTFIMI	99.9	3.9	4.1
14	AT4G36250.1 Putative aldehyde dehydrogenase	MEAMKETV	99.9	n/a	70.6
15	AT4G23710.1 Vacuolar ATP synthase subunit G2	MESAGIQQ	99.8	39.8	39.4
16	AT4G34490.1 Cyclase associated protein 1	MEEDLIKR	99.8	6.3	3.9
17	AT5G59870.1 Histone H2A 6	MESTGKVK	99.8	n/a	15.6
18	AT5G03430.1 Phosphoadenosine phosphosulfate (PAPS) reductase family protein	MEIDKAIG	99.7	2.1	3.2

19	AT5G27640.1	Eukaryotic translation initiation factor 3 subunit B	MEVVDIDA	99.7	4.2	2.5
20	AT4G23400.1	Plasma membrane intrinsic protein 1;5	MEGKEEDV	99.6	25.1	22.2
21	AT5G54310.1	ADP-ribosylation factor GTPase-activating protein AGD5	MNEKANVS	99.6	1.8	n/a
22	AT5G54430.1	Contains a universal stress protein domain	MNPADSDH	99.5	42.5	41
23	AT3G48990.1	AMP-dependent synthetase and ligase family protein	MDSDTLSG	99.4	13.9	7.9
24	AT4G11150.1	Vacuolar H ⁺ -ATPase subunit E isoform 1	MNDGDVSR	99.4	2.2	n/a
25	AT4G23730.1	Glucose-6-phosphate 1-epimerase	MEPSSGTG	99.4	62.4	61.8
26	AT4G33090.1	Aminopeptidase M1	MDQFKGEP	99.4	15.4	20.5
27	AT3G42790.1	Alfin1-like family of nuclear-localized PHD (plant homeodomain) domain containing proteins.	MEGGAALY	99.3	37	n/a
28	AT2G34160.1	Uncharacterized protein	MEEITDGV	99.2	83.3	78.3
29	AT5G10780.1	ER membrane protein complex subunit-like protein	MDK GKAVM	99.1	88.2	85.6
30	AT1G62380.1	1-aminocyclopropane-1-carboxylic oxidase (ACC oxidase)	MEKNMKFP	98.7	23.6	n/a
31	AT3G53890.1	40S ribosomal protein S21-1	MENDAGQV	98.2	5.2	12.4
32	AT1G29250.1	Alba DNA/RNA-binding protein	MEEITEGV	96.3	43.6	n/a
33	AT4G05530.1	Indole-3-butyric acid response 1	MEKKLPRR	82.2	1.9	1.6
34	AT1G20696.1	High mobility group B3 (HMGB3)	MKGAKSKA	15.9	12.3	13.1
35	AT1G20693.1	High mobility group B2 (HMGB2)	MKGAKSKT	12	7.9	8.9

737

738 **Table 3: GO term enrichment analysis for differentially regulated genes in**
 739 **NatB-depleted plants.** Total RNA was extracted from 17-day-old *naa20-1* and wild-
 740 type seedlings grown under short-day conditions (N=4). The transcripts were
 741 analyzed via an Affimetrix® GeneChip. Differentially regulated transcripts (>1.5-fold
 742 up- or downregulated compared to wild-type, $p < 0.05$) were subjected to a gene
 743 ontology enrichment analysis performed with the DAVID Bioinformatics Resources
 744 tool v.6.8 (<http://david.abcc.ncifcrf.gov>). Among the 494 differentially regulated
 745 transcripts, genes involved in the depicted molecular functions were significantly (>3-
 746 fold, $p < 0.05$) enriched. Counts represent the number of regulated transcripts. For
 747 clarity, redundant GO terms are omitted in this table; all GO terms are available in
 748 Supplementary Table 5.

Gene Ontology Term	Annotation	Count	Trend	Fold enriched	P value
defense response to bacterium	GO:0009816	6	Down	17.1	0.00
chitin metabolic/catabolic process	GO:0006030	4	Down	11.9	0.00
toxin metabolic/catabolic process	GO:0009404	5	Down	8.1	0.00
regulation of defense response	GO:0031347	6	Down	7.3	0.00
indole derivative metabolic process	GO:0042434	4	Down	7.1	0.02
polysaccharide catabolic process	GO:0000272	6	Down	6.0	0.00
response to bacterium	GO:0009617	19	Down	5.8	0.00
response to light intensity	GO:0009642	5	Down	5.1	0.02
immune response	GO:0006955	20	Down	5.1	0.00
cell death	GO:0008219	17	Down	5.0	0.00
response to chitin	GO:0010200	8	Down	4.7	0.00
response to oxidative stress	GO:0006979	15	Down	3.9	0.00
response to salicylic acid stimulus	GO:0009751	7	Down	3.5	0.02
defense response	GO:0006952	45	Down	3.2	0.00
zinc ion transport	GO:0006829	4	Up	27.9	0.00
transition metal ion transport	GO:0000041	5	Up	10.0	0.00
lipid localization	GO:0010876	7	Up	6.2	0.00
lipid transport	GO:0006869	5	Up	5.0	0.02

749

750

751 **Figure Legends**

752

753 **Figure 1. AtNatB acetylates MDEL peptides *in vitro*.** **A** Size-exclusion
754 chromatography coupled to multi-angle light scattering (SEC-MALS) analyses of
755 AtNatB. The UV-signal (blue) of the corresponding SEC chromatogram is shown
756 together with the light scattering signal (grey) and the mass distribution (red bar). The
757 experimentally determined molecular weight (MW) is 132.1 kDa and fits well to the
758 theoretical calculated molecular weight of 132.5 kDa for both subunits. **B** Substrate
759 specificity of AtNatB tested with five different peptides. The peptides SESS, EEEL,
760 MDEL, MLGTE and MVNALE were previously identified as NatA, Naa10/Naa80,
761 NatB and NatC/E/F substrates. The control reaction was performed in the absence of
762 peptides. **C** Michaelis-Menten plot of the acetylation of MDEL catalyzed by AtNatB.
763 **B-C** The reactions were performed in triplicate and error bars represent SD. **D**
764 Enzymatic parameters of AtNatB compared to its *Candida albicans* homolog
765 (CaNatB, Hong et al. (2017)).

766

767 **Figure 2. Depletion of NatB results in growth retardation.** **A** Representative
768 growth phenotypes of wild-type, *naa20-1*, and *naa25-1* plants grown for six weeks
769 under short-day conditions. Images were digitally extracted for comparison. **B** Growth
770 curve based on the rosette radius 20–79 days after stratification. **C,D** Quantification
771 of relative *NAA20* (**C**) and *NAA25* (**D**) transcript levels via RT-qPCR analysis of
772 expression in the leaves of six-week-old plants. **E** Quantification of the NAA25 protein
773 amount detected via a specific antiserum in soluble leaf protein extracts of six-week-
774 old plants grown under short-day conditions (**F**) as specified in the Materials and
775 Methods. **F** Immunological detection of AtNAA25 for quantification shown in **E** (n=4).
776 The blot shows four biological replicates for each genotype grown under identical
777 conditions. Data given as means \pm SE Different letters indicate individual groups
778 identified by pairwise multiple comparisons with a Holm-Sidak, One-way ANOVA
779 ($p < 0.05$, $n \geq 3$).

780

781 **Figure 3. The Arabidopsis *naa20-1* mutant can be complemented with the**
782 **HsNAA20 orthologue.** Representative growth phenotypes of plants grown for eight
783 weeks under short-day conditions. *naa20-1* mutant plants were transformed either
784 with **A** the endogenous Arabidopsis *NAA20* (*naa20-1:AtNAA20*) or the respective
785 homologues from humans (*naa20-1:HsNAA20*) or **B** yeast (*naa20-1:ScNAA20*).
786 Scale bar, 2 cm. Images of plants shown in panels A and B were digitally extracted
787 for comparison. **C** Relative rosette dry weight of the indicated plants after eight weeks
788 of growth. For each transformation, three representative independent lines are
789 shown. Data given as means \pm SE. Different letters indicate individual groups
790 identified by pairwise multiple comparisons with a Holm-Sidak, One-way ANOVA
791 ($p < 0.05$, $n \geq 3$).

792

793 **Figure 4. The Arabidopsis NatB complex acetylates N-termini which retain their**
794 **iMet. A-C** The acetylation level of protein N-termini was studied in leaves of six-
795 week-old plants grown under short-day conditions on soil. The mass spectrometry
796 analysis depicts the acetylation levels of all detected N-termini (**A**) as well as N-
797 termini with (**B**) or without (**C**) N-terminal methionine excision (NME). **D** Based on the
798 identified substrates, the NatB target consensus sequence was determined using
799 weblogo.berkeley.edu. The size of the letter code corresponds to the relative amino
800 acid frequency at positions one to ten. **E** Quantification of the relative global amount
801 of free N-termini in soluble protein extracts isolated from leaves of six-week-old
802 plants. Data given as means \pm SE. Different letters indicate individual groups
803 identified by pairwise multiple comparisons with a Holm-Sidak, One-way ANOVA
804 ($p < 0.05$, $n \geq 3$). **F** Section of 2D-PAGE gels comparing soluble protein extracts of nine-
805 week-old wild-type and *naa20-1* plants. Arrows mark proteins with a basic shift in the
806 *naa20-1* mutant, indicating a loss of NTA. Proteins were identified by mass
807 spectrometry. 1/1* salt stress-related protein (AT1G13930, MD), 2/2* nucleoside
808 diphosphate kinase 1 (AT4G09320, ME), 3/3* membrane-associated progesterone
809 binding protein (AT2G24940, ME).

810

811 **Figure 5. NatB mutants are sensitive to salt and osmotic stress.** Seeds of
812 mutants depleted in subunits of NatB or NatA were surface sterilized, stratified for
813 two days and germinated on 1xMS medium (Control) or medium supplemented with
814 100 mM NaCl (NaCl) or 3% mannitol (Mannitol), respectively. Germination of plants
815 was evaluated after seven days of growth under short-day conditions. **A, B**
816 Representative sections of germinated and non-germinated seeds. Scale bars, 5 mm.
817 **C, D** Quantification of corresponding germination rates. Data given as means \pm SE.
818 Different letters indicate individual groups identified by pairwise multiple comparisons
819 with a Holm-Sidak, One-way ANOVA ($p < 0.05$, $n = 3$, $1n \geq 30$ seeds).

820

821 References

- 822 **Aksnes H, Drazic A, Marie M, Arnesen T** (2016) First Things First: Vital Protein Marks by N-Terminal
823 Acetyltransferases. *Trends Biochem Sci* **41**: 746-760
- 824 **Aksnes H, Hole K, Arnesen T** (2015a) Molecular, cellular, and physiological significance of N-terminal
825 acetylation. *Int Rev Cell Mol Biol* **316**: 267-305
- 826 **Aksnes H, Ree R, Arnesen T** (2019) Co-translational, Post-translational, and Non-catalytic Roles of N-
827 Terminal Acetyltransferases. *Mol Cell* **73**: 1097-1114
- 828 **Aksnes H, Van Damme P, Goris M, Starheim KK, Marie M, Stove SI, Hoel C, Kalvik TV, Hole K,**
829 **Glomnes N, Furnes C, Ljostveit S, Ziegler M, Niere M, Gevaert K, Arnesen T** (2015b) An
830 organellar alpha-acetyltransferase, *naa60*, acetylates cytosolic N termini of transmembrane
831 proteins and maintains Golgi integrity. *Cell Rep* **10**: 1362-1374
- 832 **Alexander MP** (1969) Differential staining of aborted and nonaborted pollen. *Stain Technol* **44**: 117-
833 122
- 834 **Alonso JM, Stepanova AN, Leisse TJ, Kim CJ, Chen H, Shinn P, Stevenson DK, Zimmerman J, Barajas**
835 **P, Cheuk R, Gadrinab C, Heller C, Jeske A, Koesema E, Meyers CC, Parker H, Prednis L,**
836 **Ansari Y, Choy N, Deen H, Geralt M, Hazari N, Hom E, Karnes M, Mulholland C, Ndubaku R,**
837 **Schmidt I, Guzman P, Aguilar-Henonin L, Schmid M, Weigel D, Carter DE, Marchand T,**
838 **Risseuw E, Brogden D, Zeko A, Crosby WL, Berry CC, Ecker JR** (2003) Genome-wide
839 insertional mutagenesis of *Arabidopsis thaliana*. *Science* **301**: 653-657

840 **Ametzazurra A, Gazquez C, Lasa M, Larrea E, Prieto J, Aldabe R** (2009) Characterization of the
841 human N-alpha-terminal acetyltransferase B enzymatic complex. *BMC Proc* **3 Suppl 6**: S4
842 **Ametzazurra A, Larrea E, Civeira MP, Prieto J, Aldabe R** (2008) Implication of human N-alpha-
843 acetyltransferase 5 in cellular proliferation and carcinogenesis. *Oncogene* **27**: 7296-7306
844 **Arnesen T** (2011) Towards a functional understanding of protein N-terminal acetylation. *PLoS Biol* **9**:
845 e1001074
846 **Arnesen T, Gromyko D, Kagabo D, Betts MJ, Starheim KK, Varhaug JE, Anderson D, Lillehaug JR**
847 (2009a) A novel human NatA N-alpha-terminal acetyltransferase complex: hNaa16p-hNaa10p
848 (hNat2-hArd1). *BMC Biochem* **10**: 15
849 **Arnesen T, Van Damme P, Polevoda B, Helsens K, Evjenth R, Colaert N, Varhaug JE,**
850 **Vandekerckhove J, Lillehaug JR, Sherman F, Gevaert K** (2009b) Proteomics analyses reveal
851 the evolutionary conservation and divergence of N-terminal acetyltransferases from yeast
852 and humans. *Proc Natl Acad Sci U S A* **106**: 8157-8162
853 **Bernal-Perez LF, Prokai L, Ryu Y** (2012) Selective N-terminal fluorescent labeling of proteins using 4-
854 chloro-7-nitrobenzofurazan: A method to distinguish protein N-terminal acetylation.
855 *Analytical Biochemistry* **428**: 13-15
856 **Bienvenut WV, Giglione C, Meinnel T** (2017a) SILProNAQ: A Convenient Approach for Proteome-
857 Wide Analysis of Protein N-Termini and N-Terminal Acetylation Quantitation. *Methods Mol*
858 *Biol* **1574**: 17-34
859 **Bienvenut WV, Scarpelli JP, Dumestier J, Meinnel T, Giglione C** (2017b) EnCOUNTER: a parsing tool
860 to uncover the mature N-terminus of organelle-targeted proteins in complex samples. *BMC*
861 *Bioinformatics* **18**: 182
862 **Bienvenut WV, Sumpton D, Martinez A, Lilla S, Espagne C, Meinnel T, Giglione C** (2012)
863 Comparative Large Scale Characterization of Plant versus Mammal Proteins Reveals Similar
864 and Idiosyncratic N- α -Acetylation Features. *Molecular & Cellular Proteomics* **11**:
865 M111.015131
866 **Blum H, Beier H, Gross HJ** (1987) Improved silver staining of plant proteins, RNA and DNA in
867 polyacrylamide gels. *Electrophoresis* **8**: 93-99
868 **Bradford MM** (1976) A rapid and sensitive method for the quantitation of microgram quantities of
869 protein utilizing the principle of protein-dye binding. *Anal Biochem* **72**: 248-254
870 **Caesar R, Blomberg A** (2004) The stress-induced Tfs1p requires NatB-mediated acetylation to inhibit
871 carboxypeptidase Y and to regulate the protein kinase A pathway. *J Biol Chem* **279**: 38532-
872 38543
873 **Caesar R, Warringer J, Blomberg A** (2006) Physiological importance and identification of novel
874 targets for the N-terminal acetyltransferase NatB. *Eukaryot Cell* **5**: 368-378
875 **Casey JP, Støve SI, McGorrian C, Galvin J, Blenski M, Dunne A, Ennis S, Brett F, King MD, Arnesen T,**
876 **Lynch SA** (2015) NAA10 mutation causing a novel intellectual disability syndrome with Long
877 QT due to N-terminal acetyltransferase impairment. *Scientific Reports* **5**: 16022
878 **Chen Z, Zhao P-X, Miao Z-Q, Qi G-F, Wang Z, Yuan Y, Ahmad N, Cao M-J, Hell R, Wirtz M, Xiang C-B**
879 (2019) SULTR3s Function in Chloroplast Sulfate Uptake and Affect ABA Biosynthesis and the
880 Stress Response. *Plant Physiol* **180**: 593-604
881 **Czechowski T, Stitt M, Altmann T, Udvardi MK, Scheible WR** (2005) Genome-wide identification and
882 testing of superior reference genes for transcript normalization in Arabidopsis. *Plant Physiol*
883 **139**: 5-17
884 **Dinh TV, Bienvenut WV, Linster E, Feldman-Salit A, Jung VA, Meinnel T, Hell R, Giglione C, Wirtz M**
885 (2015) Molecular identification and functional characterization of the first N^a-
886 acetyltransferase in plastids by global acetylome profiling. *Proteomics* **15**: 2426-2435
887 **Drazic A, Aksnes H, Marie M, Boczkowska M, Varland S, Timmerman E, Foyen H, Glomnes N,**
888 **Rebowski G, Impens F, Gevaert K, Dominguez R, Arnesen T** (2018) NAA80 is actin's N-
889 terminal acetyltransferase and regulates cytoskeleton assembly and cell motility. *Proc Natl*
890 *Acad Sci U S A*
891 **Dupree P, Sherrier DJ** (1998) The plant Golgi apparatus. *Biochim Biophys Acta* **1404**: 259-270

892 **Falb M, Aivaliotis M, Garcia-Rizo C, Bisle B, Tebbe A, Klein C, Konstantinidis K, Siedler F, Pfeiffer F,**
893 **Oesterhelt D** (2006) Archaeal N-terminal protein maturation commonly involves N-terminal
894 acetylation: a large-scale proteomics survey. *J Mol Biol* **362**: 915-924

895 **Ferrandez-Ayela A, Micol-Ponce R, Sanchez-García AB, Alonso-Peral MM, Micol JL, Ponce MR**
896 (2013) Mutation of an Arabidopsis NatB N-Alpha-Terminal Acetylation Complex Component
897 Causes Pleiotropic Developmental Defects. *PLoS ONE* **8**: e80697, 80691-80611

898 **Frottin F, Martinez A, Peynot P, Mitra S, Holz RC, Giglione C, Meinnel T** (2006) The proteomics of N-
899 terminal methionine cleavage. *Mol Cell Proteomics* **5**: 2336-2349

900 **Giglione C, Fiulaine S, Meinnel T** (2015) N-terminal protein modifications: Bringing back into play
901 the ribosome. *Biochimie*

902 **Heeg C, Kruse C, Jost R, Gutensohn M, Ruppert T, Wirtz M, Hell R** (2008) Analysis of the Arabidopsis
903 *O*-acetylserine(thiol)lyase gene family demonstrates compartment-specific differences in the
904 regulation of cysteine synthesis. *Plant Cell* **20**: 168-185

905 **Helbig AO, Rosati S, Pijnappel PW, van Breukelen B, Timmers MH, Mohammed S, Slijper M, Heck AJ**
906 (2010) Perturbation of the yeast N-acetyltransferase NatB induces elevation of protein
907 phosphorylation levels. *BMC Genomics* **11**: 685

908 **Hong H, Cai Y, Zhang S, Ding H, Wang H, Han A** (2017) Molecular Basis of Substrate Specific
909 Acetylation by N-Terminal Acetyltransferase NatB. *Structure* **25**: 641-649 e643

910 **Huang da W, Sherman BT, Lempicki RA** (2009a) Bioinformatics enrichment tools: paths toward the
911 comprehensive functional analysis of large gene lists. *Nucleic Acids Res* **37**: 1-13

912 **Huang da W, Sherman BT, Lempicki RA** (2009b) Systematic and integrative analysis of large gene lists
913 using DAVID bioinformatics resources. *Nat Protoc* **4**: 44-57

914 **Kaundal R, Saini R, Zhao PX** (2010) Combining Machine Learning and Homology-Based Approaches
915 to Accurately Predict Subcellular Localization in Arabidopsis. *Plant Physiology* **154**: 36-54

916 **Linster E, Stephan I, Bienvenut WV, Maple-Grodem J, Myklebust LM, Huber M, Reichelt M, Sticht C,**
917 **Geir Moller S, Meinnel T, Arnesen T, Giglione C, Hell R, Wirtz M** (2015) Downregulation of
918 N-terminal acetylation triggers ABA-mediated drought responses in Arabidopsis. *Nat*
919 *Commun* **6**: 7640

920 **Linster E, Wirtz M** (2018) N-terminal acetylation: an essential protein modification emerges as an
921 important regulator of stress responses. *J Exp Bot* **69**: 4555-4568

922 **Nguyen KT, Kim JM, Park SE, Hwang CS** (2019) N-terminal methionine excision of proteins creates
923 tertiary destabilizing N-degrons of the Arg/N-end rule pathway. *J Biol Chem* **294**: 4464-4476

924 **Nilsson OB, Hedman R, Marino J, Wickles S, Bischoff L, Johansson M, Muller-Lucks A, Trovato F,**
925 **Puglisi JD, O'Brien EP, Beckmann R, von Heijne G** (2015) Cotranslational Protein Folding
926 inside the Ribosome Exit Tunnel. *Cell Rep* **12**: 1533-1540

927 **Noji M, Inoue K, Kimura N, Gouda A, Saito K** (1998) Isoform-dependent differences in feedback
928 regulation and subcellular localization of serine acetyltransferase involved in cysteine
929 biosynthesis from Arabidopsis thaliana. *J Biol Chem* **273**: 32739-32745

930 **Pesaresi P, Gardner NA, Masiero S, Dietzmann A, Eichacker L, Wickner R, Salamini F, Leister D**
931 (2003) Cytoplasmic N-terminal protein acetylation is required for efficient photosynthesis in
932 Arabidopsis. *Plant Cell* **15**: 1817-1832

933 **Pierre M, Traverso JA, Boisson B, Domenichini S, Bouchez D, Giglione C, Meinnel T** (2007) N-
934 myristoylation regulates the SnRK1 pathway in Arabidopsis. *Plant Cell* **19**: 2804-2821

935 **Polevoda B, Arnesen T, Sherman F** (2009) A synopsis of eukaryotic Nalpha-terminal
936 acetyltransferases: nomenclature, subunits and substrates. *BMC Proc* **3 Suppl 6**: S2

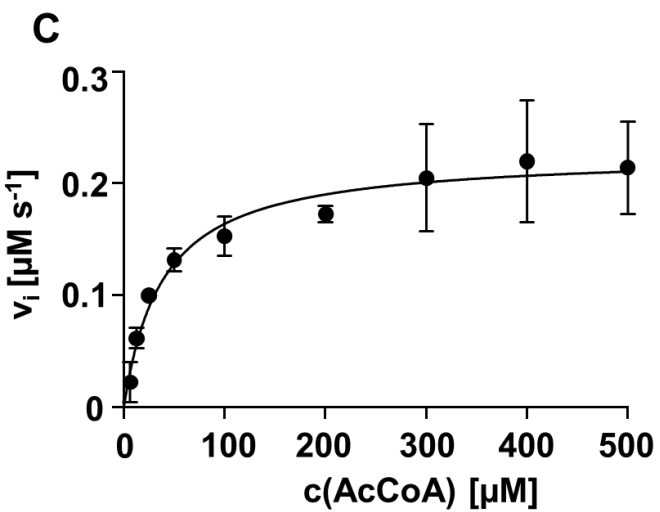
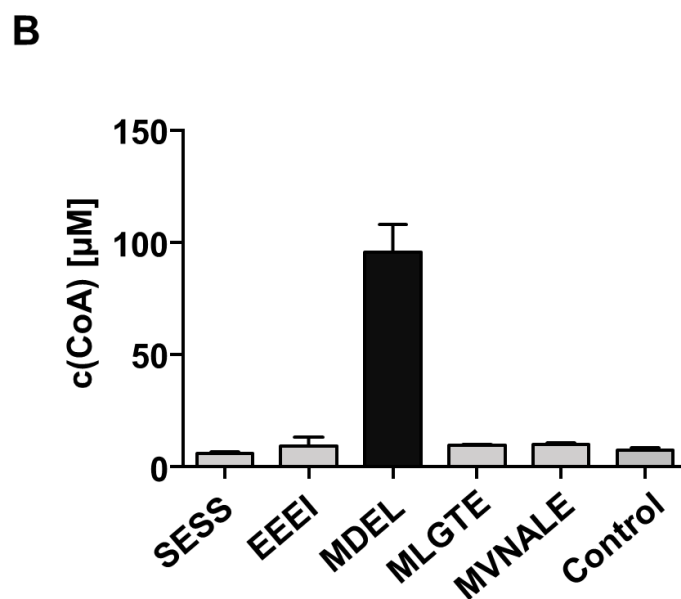
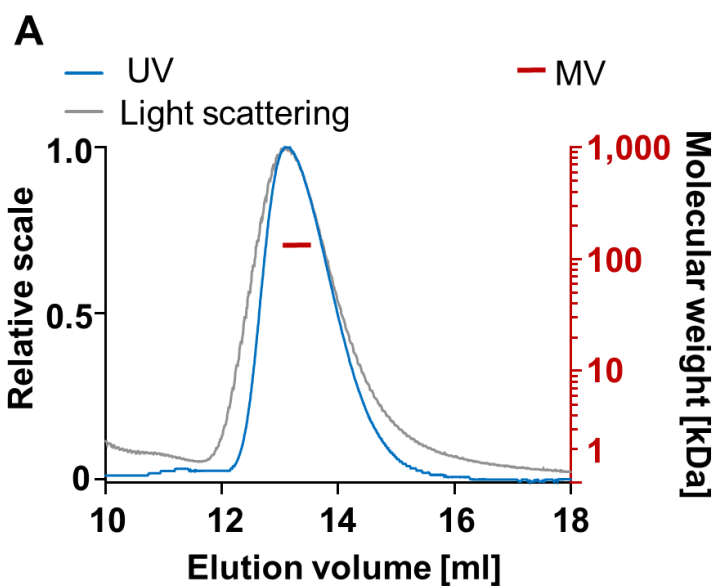
937 **Polevoda B, Brown S, Cardillo TS, Rigby S, Sherman F** (2008) Yeast N(alpha)-terminal
938 acetyltransferases are associated with ribosomes. *J Cell Biochem* **103**: 492-508

939 **Polevoda B, Cardillo TS, Doyle TC, Bedi GS, Sherman F** (2003) Nat3p and Mdm20p are required for
940 function of yeast NatB Nalpha-terminal acetyltransferase and of actin and tropomyosin. *J Biol*
941 *Chem* **278**: 30686-30697

942 **Polevoda B, Sherman F** (2003) N-terminal acetyltransferases and sequence requirements for N-
943 terminal acetylation of eukaryotic proteins. *J Mol Biol* **325**: 595-622

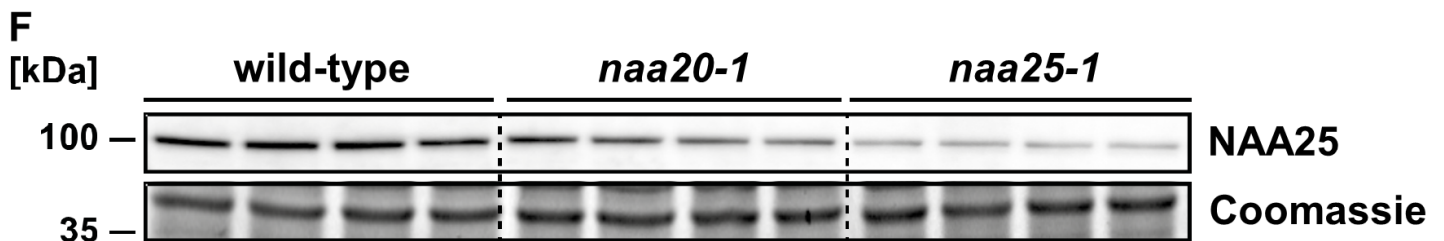
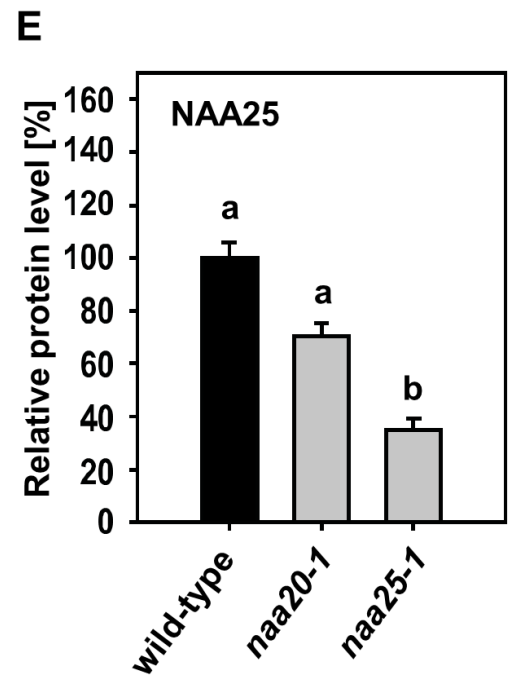
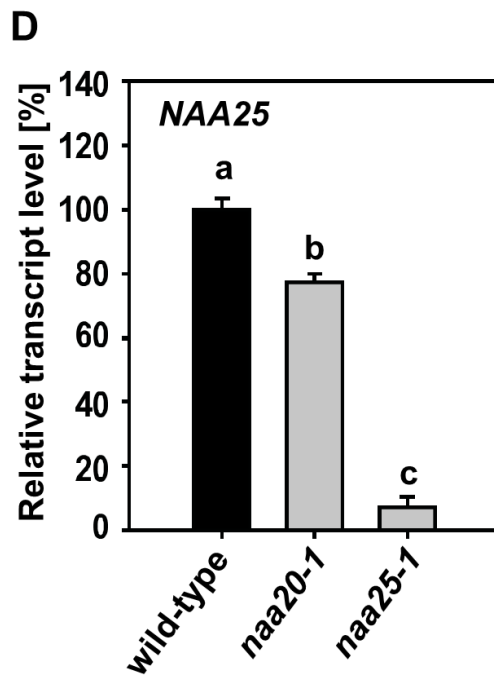
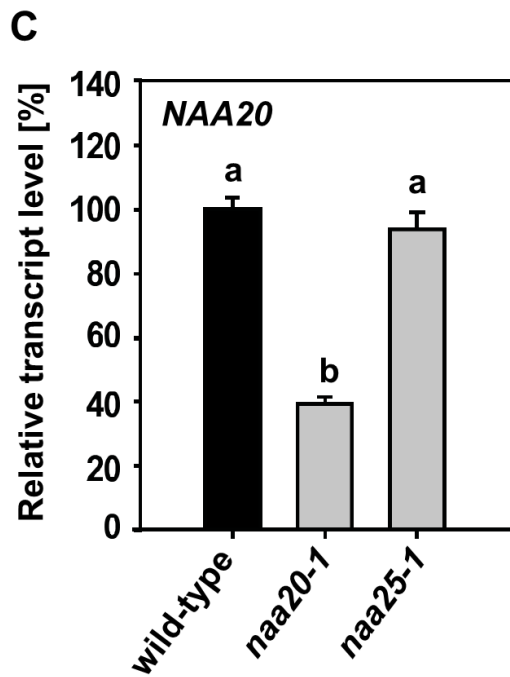
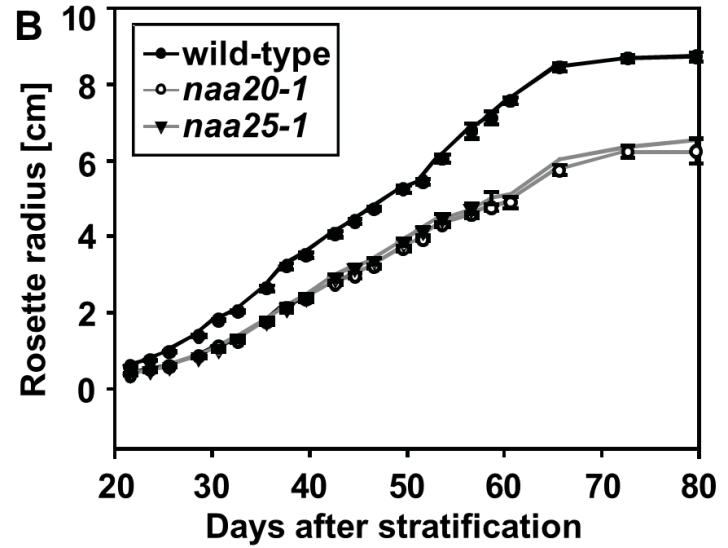
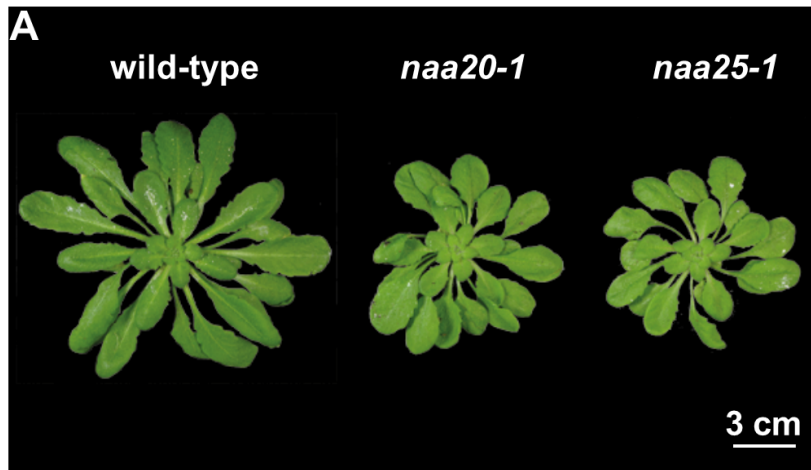
944 **Ree R, Myklebust LM, Thiel P, Foyn H, Fladmark KE, Arnesen T** (2015) The N-terminal
945 acetyltransferase Naa10 is essential for zebrafish development. *Biosci Rep* **35**
946 **Reid DW, Nicchitta CV** (2015) Diversity and selectivity in mRNA translation on the endoplasmic
947 reticulum. *Nature reviews. Molecular cell biology* **16**: 221-231
948 **Rosso MG, Li Y, Strizhov N, Reiss B, Dekker K, Weisshaar B** (2003) An *Arabidopsis thaliana* T-DNA
949 mutagenized population (GABI-Kat) for flanking sequence tag-based reverse genetics. *Plant*
950 *Mol Biol* **53**: 247-259
951 **Sessions A, Burke E, Presting G, Aux G, McElver J, Patton D, Dietrich B, Ho P, Bacwaden J, Ko C,**
952 **Clarke JD, Cotton D, Bullis D, Snell J, Miguel T, Hutchison D, Kimmerly B, Mitzel T, Katagiri F,**
953 **Glazebrook J, Law M, Goff SA** (2002) A high-throughput *Arabidopsis* reverse genetics system.
954 *Plant Cell* **14**: 2985-2994
955 **Singer JM, Shaw JM** (2003) Mdm20 protein functions with Nat3 protein to acetylate Tpm1 protein
956 and regulate tropomyosin-actin interactions in budding yeast. *Proc Natl Acad Sci U S A* **100**:
957 7644-7649
958 **Starheim KK, Arnesen T, Gromyko D, Rynningen A, Varhaug JE, Lillehaug JR** (2008) Identification of
959 the human N(alpha)-acetyltransferase complex B (hNatB): a complex important for cell-cycle
960 progression. *Biochem J* **415**: 325-331
961 **Van Damme P, Lasa M, Polevoda B, Gazquez C, Elosegui-Artola A, Kim DS, De Juan-Pardo E,**
962 **Demeyer K, Hole K, Larrea E, Timmerman E, Prieto J, Arnesen T, Sherman F, Gevaert K,**
963 **Aldabe R** (2012) N-terminal acetylome analyses and functional insights of the N-terminal
964 acetyltransferase NatB. *Proc Natl Acad Sci U S A* **109**: 12449-12454
965 **Xu F, Huang Y, Li L, Gannon P, Linster E, Huber M, Kapos P, Bienvenut W, Polevoda B, Meinel T,**
966 **Hell R, Giglione C, Zhang Y, Wirtz M, Chen S, Li X** (2015) Two N-terminal acetyltransferases
967 antagonistically regulate the stability of a nod-like receptor in *Arabidopsis*. *Plant Cell* **27**:
968 1547-1562

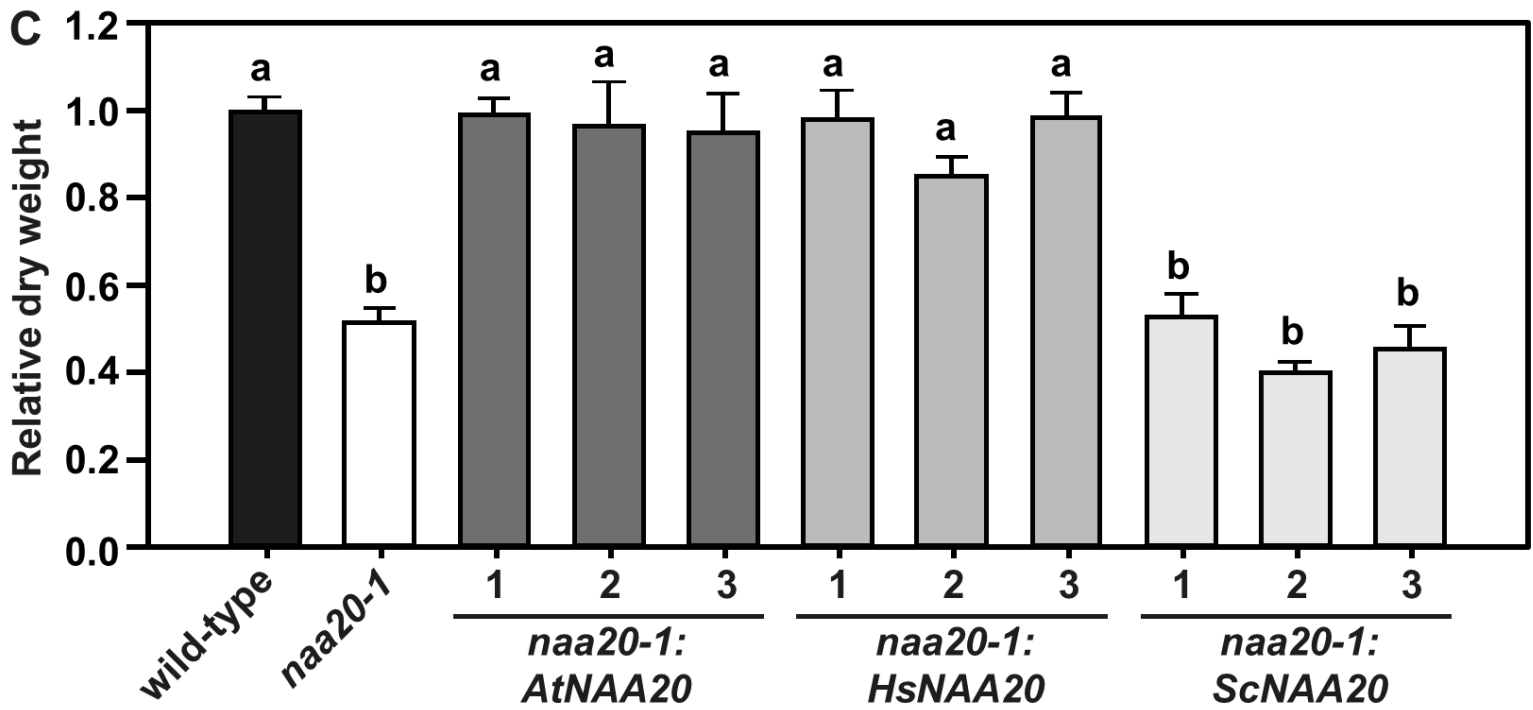
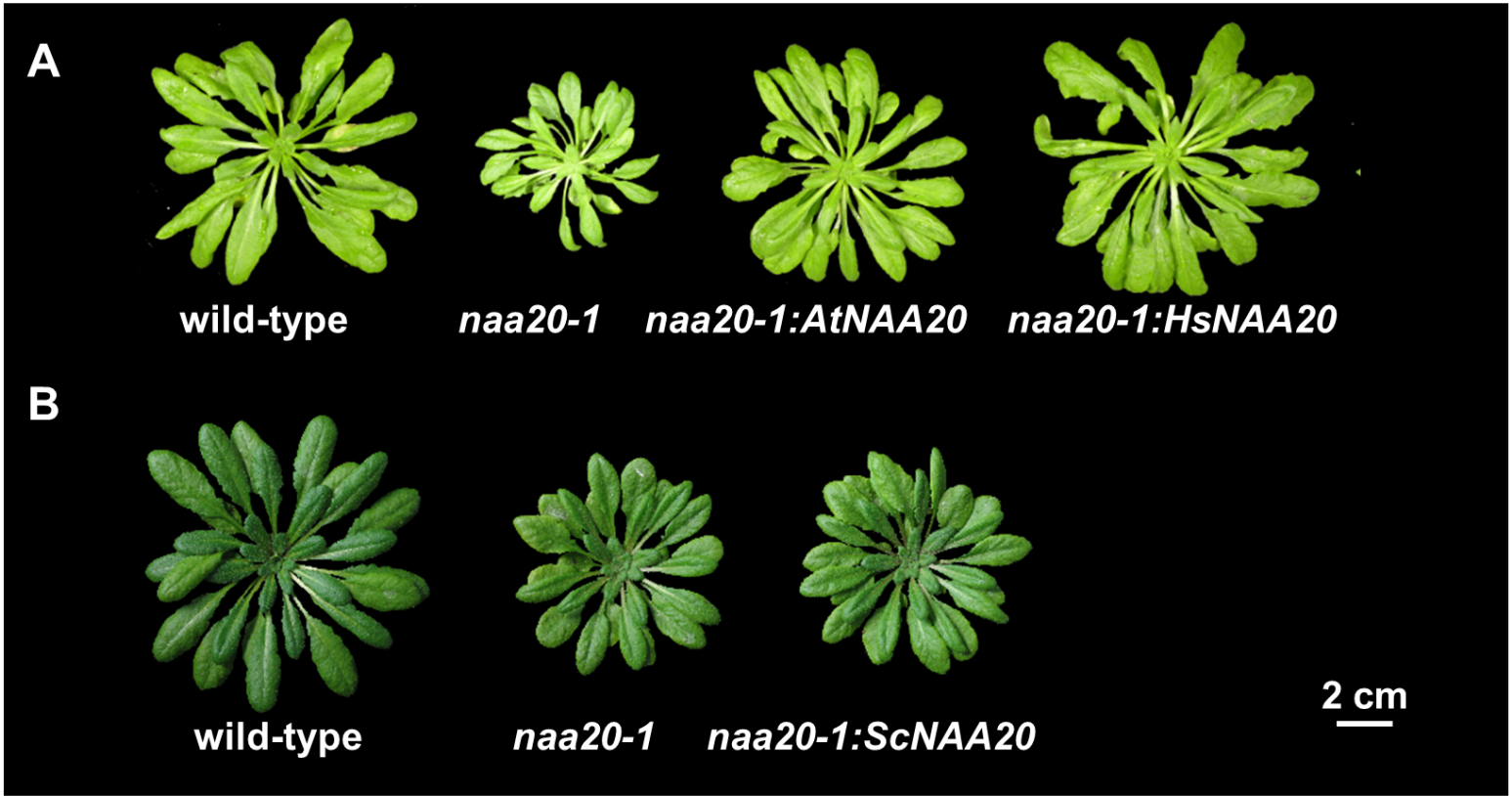
969

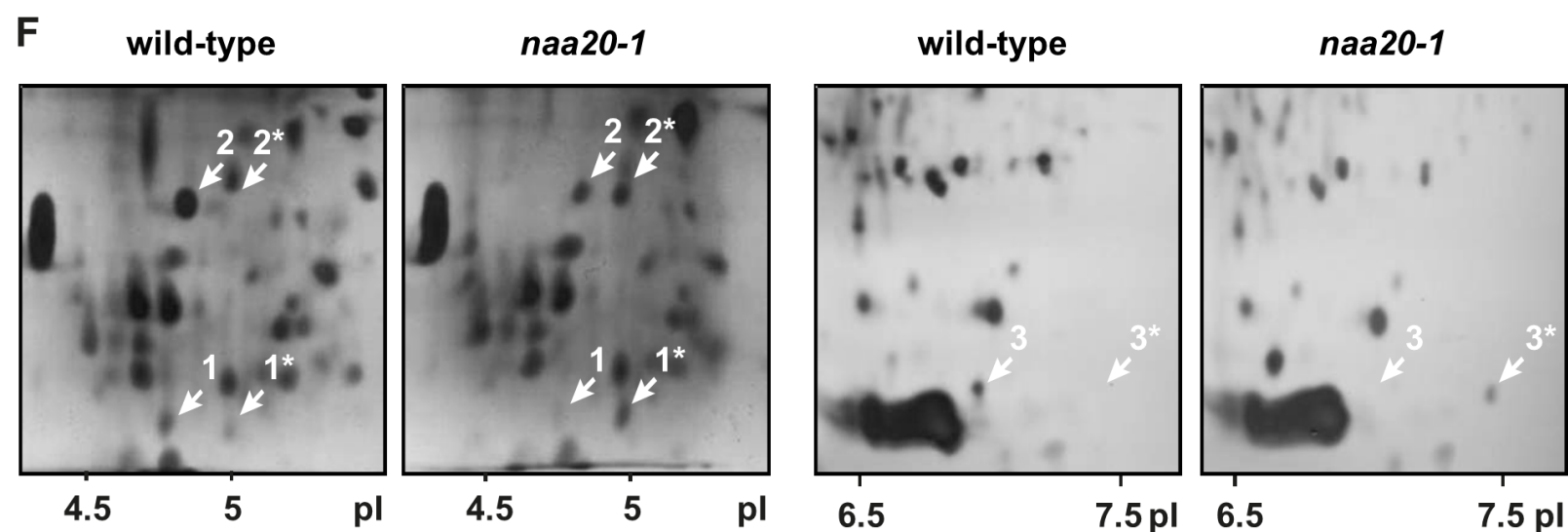
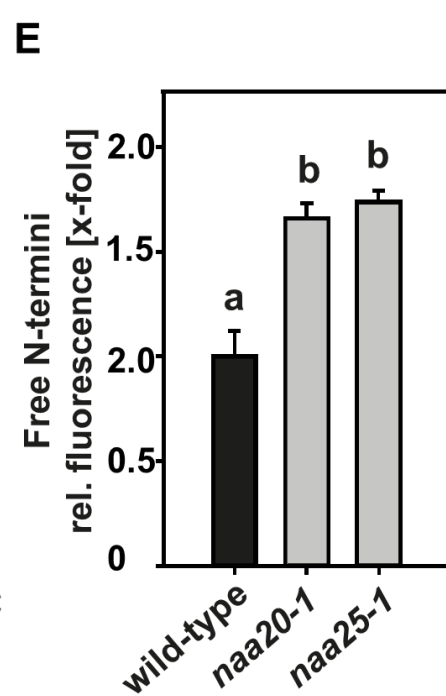
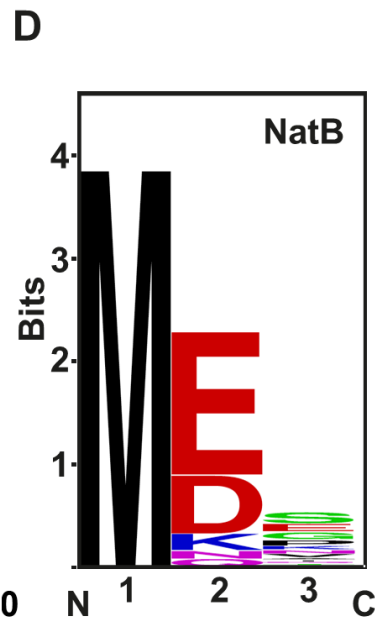
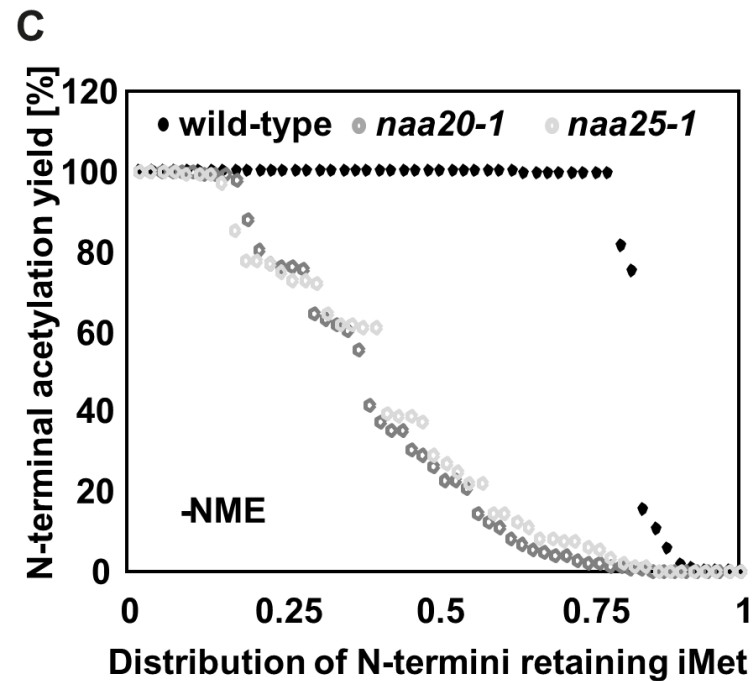
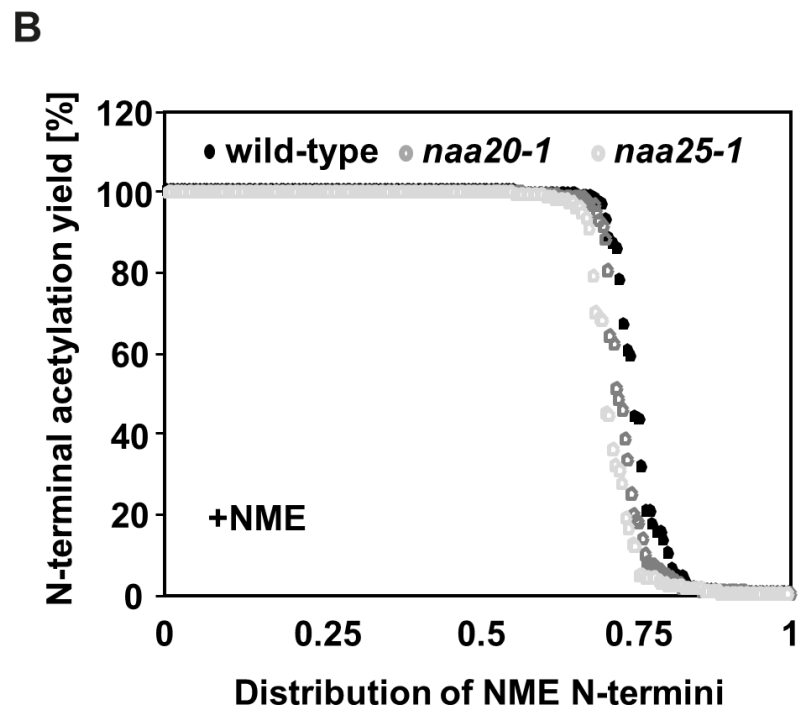
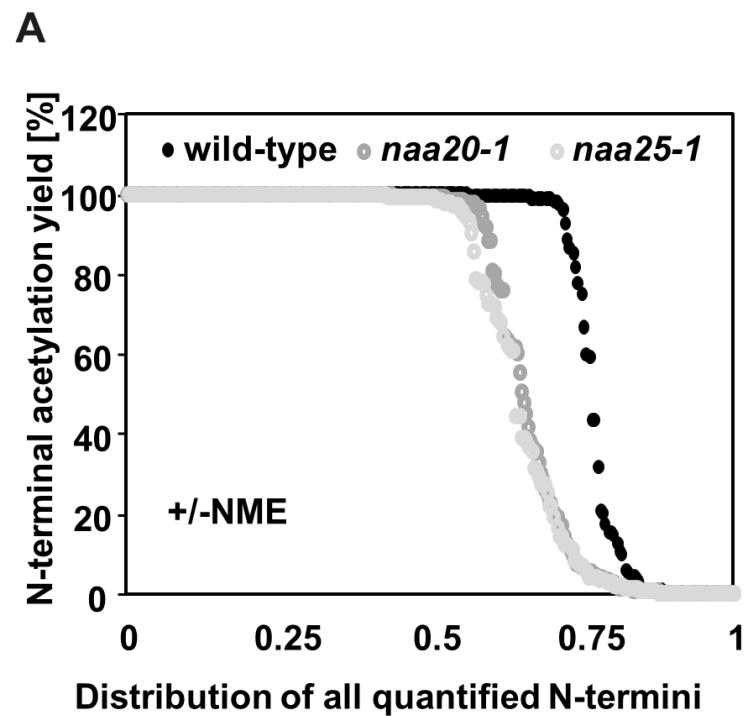


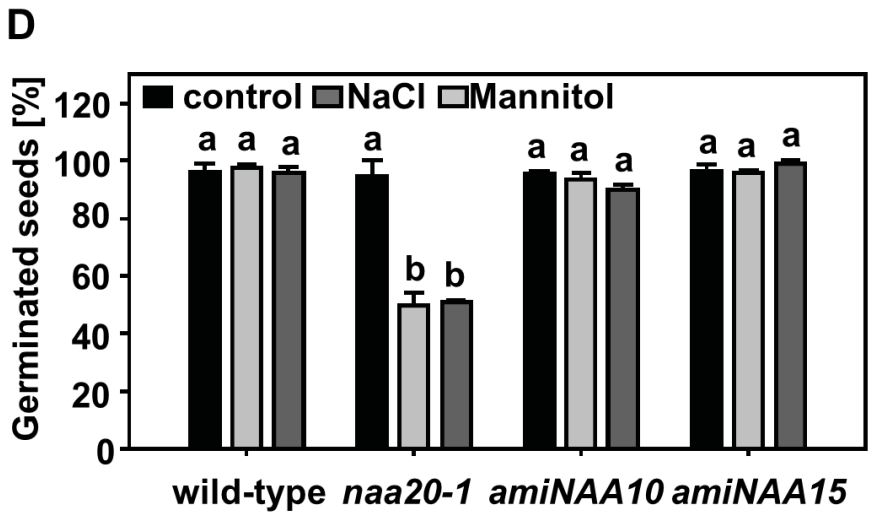
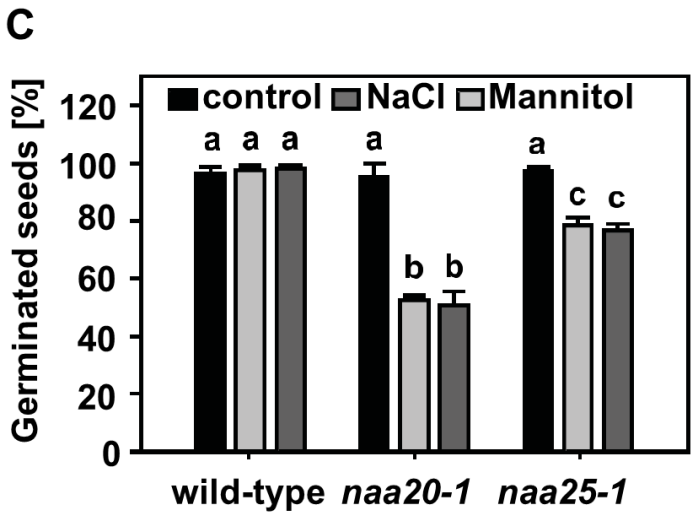
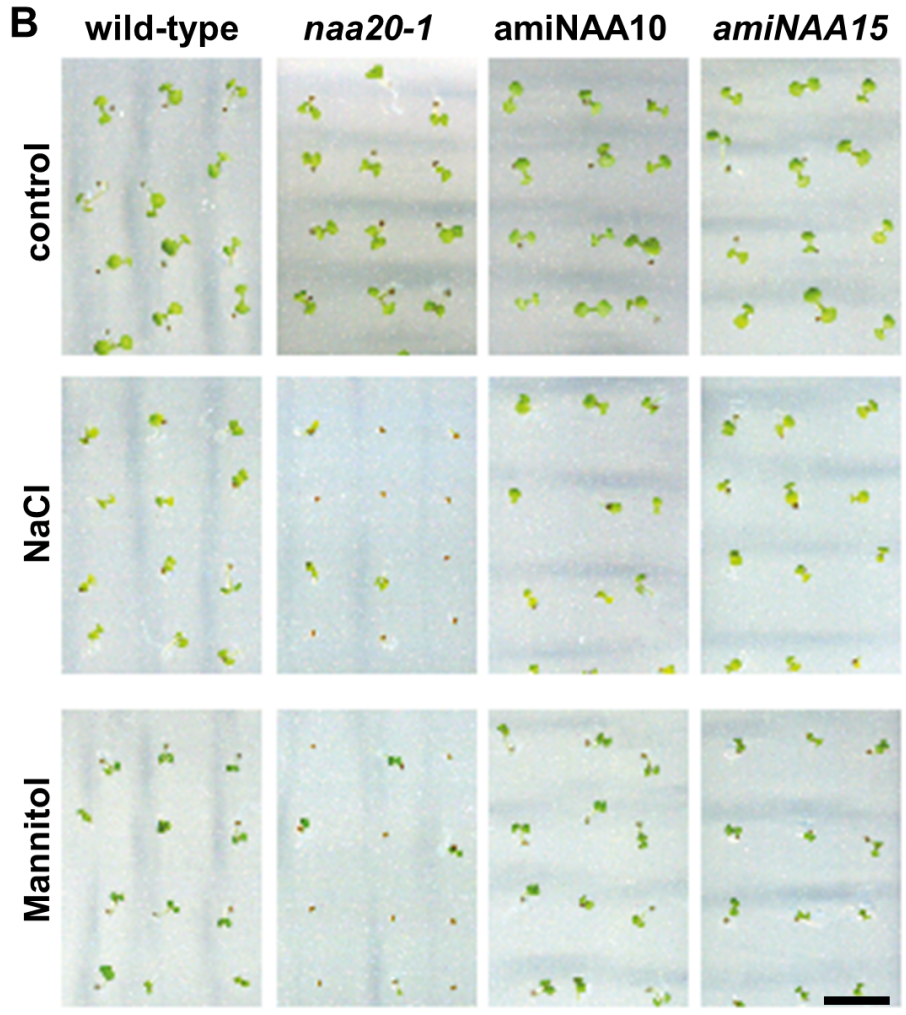
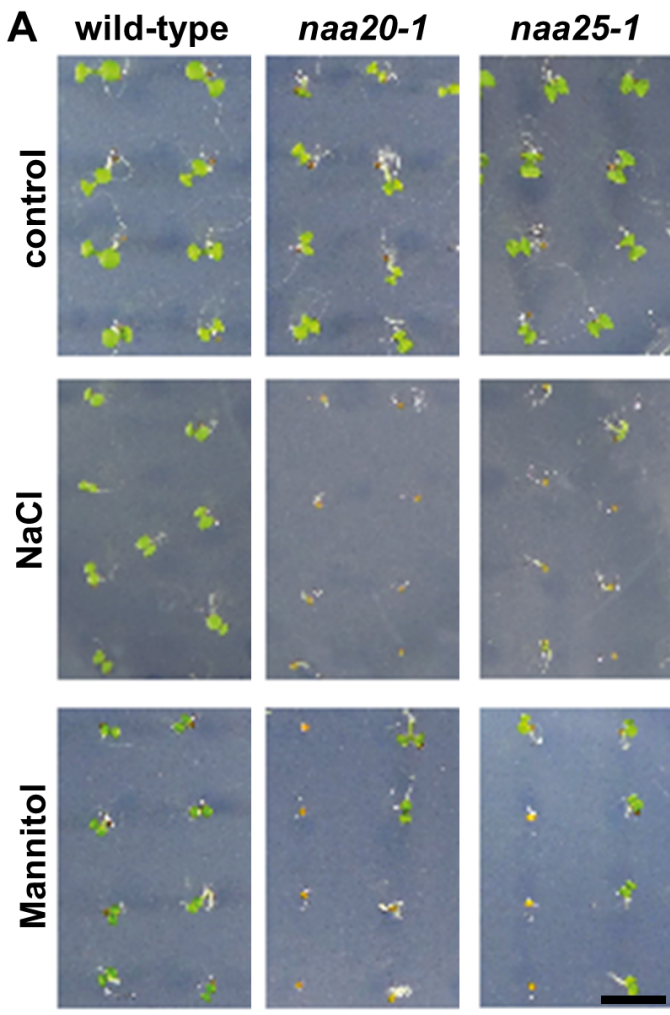
D

Parameter	<i>At</i> NatB	<i>Ca</i> NatB
K_m (μM)	38.4 ± 9.1	50.0 ± 8.0
k_{cat} (min ⁻¹)	27.3 ± 1.6	63.3 ± 3.0
k_{cat}/K_m (min ⁻¹ μM ⁻¹)	0.71 ± 0.15	1.27 ± 0.21









Parsed Citations

Aksnes H, Drazic A, Marie M, Arnesen T (2016) First Things First: Vital Protein Marks by N-Terminal Acetyltransferases. Trends Biochem Sci 41: 746-760

Pubmed: [Author and Title](#)

Google Scholar: [Author Only Title Only Author and Title](#)

Aksnes H, Hole K, Arnesen T (2015a) Molecular, cellular, and physiological significance of N-terminal acetylation. Int Rev Cell Mol Biol 316: 267-305

Pubmed: [Author and Title](#)

Google Scholar: [Author Only Title Only Author and Title](#)

Aksnes H, Ree R, Arnesen T (2019) Co-translational, Post-translational, and Non-catalytic Roles of N-Terminal Acetyltransferases. Mol Cell 73: 1097-1114

Pubmed: [Author and Title](#)

Google Scholar: [Author Only Title Only Author and Title](#)

Aksnes H, Van Damme P, Goris M, Starheim KK, Marie M, Stove SI, Hoel C, Kalvik TV, Hole K, Glomnes N, Furnes C, Ljostveit S, Ziegler M, Niere M, Gevaert K, Arnesen T (2015b) An organellar alpha-acetyltransferase, naa60, acetylates cytosolic N termini of transmembrane proteins and maintains Golgi integrity. Cell Rep 10: 1362-1374

Pubmed: [Author and Title](#)

Google Scholar: [Author Only Title Only Author and Title](#)

Alexander MP (1969) Differential staining of aborted and nonaborted pollen. Stain Technol 44: 117-122

Pubmed: [Author and Title](#)

Google Scholar: [Author Only Title Only Author and Title](#)

Alonso JM, Stepanova AN, Leisse TJ, Kim CJ, Chen H, Shinn P, Stevenson DK, Zimmerman J, Barajas P, Cheuk R, Gadrinab C, Heller C, Jeske A, Koesema E, Meyers CC, Parker H, Prednis L, Ansari Y, Choy N, Deen H, Geralt M, Hazari N, Hom E, Karnes M, Mulholland C, Ndubaku R, Schmidt I, Guzman P, Aguilar-Henonin L, Schmid M, Weigel D, Carter DE, Marchand T, Risseuw E, Brogden D, Zeko A, Crosby WL, Berry CC, Ecker JR (2003) Genome-wide insertional mutagenesis of Arabidopsis thaliana. Science 301: 653-657

Pubmed: [Author and Title](#)

Google Scholar: [Author Only Title Only Author and Title](#)

Ametzazurra A, Gazquez C, Lasa M, Larrea E, Prieto J, Aldabe R (2009) Characterization of the human Nalpa-terminal acetyltransferase B enzymatic complex. BMC Proc 3 Suppl 6: S4

Pubmed: [Author and Title](#)

Google Scholar: [Author Only Title Only Author and Title](#)

Ametzazurra A, Larrea E, Civeira MP, Prieto J, Aldabe R (2008) Implication of human N-alpha-acetyltransferase 5 in cellular proliferation and carcinogenesis. Oncogene 27: 7296-7306

Pubmed: [Author and Title](#)

Google Scholar: [Author Only Title Only Author and Title](#)

Arnesen T (2011) Towards a functional understanding of protein N-terminal acetylation. PLoS Biol 9: e1001074

Pubmed: [Author and Title](#)

Google Scholar: [Author Only Title Only Author and Title](#)

Arnesen T, Gromyko D, Kagabo D, Betts MJ, Starheim KK, Varhaug JE, Anderson D, Lillehaug JR (2009a) A novel human NatA Nalpa-terminal acetyltransferase complex: hNaa16p-hNaa10p (hNat2-hArd1). BMC Biochem 10: 15

Pubmed: [Author and Title](#)

Google Scholar: [Author Only Title Only Author and Title](#)

Arnesen T, Van Damme P, Polevoda B, Helsens K, Evjenth R, Colaert N, Varhaug JE, Vandekerckhove J, Lillehaug JR, Sherman F, Gevaert K (2009b) Proteomics analyses reveal the evolutionary conservation and divergence of N-terminal acetyltransferases from yeast and humans. Proc Natl Acad Sci U S A 106: 8157-8162

Pubmed: [Author and Title](#)

Google Scholar: [Author Only Title Only Author and Title](#)

Bernal-Perez LF, Prokai L, Ryu Y (2012) Selective N-terminal fluorescent labeling of proteins using 4-chloro-7-nitrobenzofurazan: A method to distinguish protein N-terminal acetylation. Analytical Biochemistry 428: 13-15

Pubmed: [Author and Title](#)

Google Scholar: [Author Only Title Only Author and Title](#)

Bienvenut WW, Giglione C, Meinnel T (2017a) SILProNAQ: A Convenient Approach for Proteome-Wide Analysis of Protein N-Termini and N-Terminal Acetylation Quantitation. Methods Mol Biol 1574: 17-34

Pubmed: [Author and Title](#)

Google Scholar: [Author Only Title Only Author and Title](#)

Bienvenut WW, Scarpelli JP, Dumestier J, Meinnel T, Giglione C (2017b) EnCOUNTER: a parsing tool to uncover the mature N-terminus of organelle-targeted proteins in complex samples. BMC Bioinformatics 18: 182

Pubmed: [Author and Title](#)

Google Scholar: [Author Only Title Only Author and Title](#)

Bienvenut WW, Sumpton D, Martinez A, Lilla S, Espagne C, Meinel T, Giglione C (2012) Comparative Large Scale Characterization of Plant versus Mammal Proteins Reveals Similar and Idiosyncratic N- α -Acetylation Features. *Molecular & Cellular Proteomics* 11: M111.015131

Pubmed: [Author and Title](#)

Google Scholar: [Author Only Title Only Author and Title](#)

Blum H, Beier H, Gross HJ (1987) Improved silver staining of plant proteins, RNA and DNA in polyacrylamide gels. *Electrophoresis* 8: 93-99

Pubmed: [Author and Title](#)

Google Scholar: [Author Only Title Only Author and Title](#)

Bradford MM (1976) A rapid and sensitive method for the quantitation of microgram quantities of protein utilizing the principle of protein-dye binding. *Anal Biochem* 72: 248-254

Pubmed: [Author and Title](#)

Google Scholar: [Author Only Title Only Author and Title](#)

Caesar R, Blomberg A (2004) The stress-induced Tfs1p requires NatB-mediated acetylation to inhibit carboxypeptidase Y and to regulate the protein kinase A pathway. *J Biol Chem* 279: 38532-38543

Pubmed: [Author and Title](#)

Google Scholar: [Author Only Title Only Author and Title](#)

Caesar R, Warringer J, Blomberg A (2006) Physiological importance and identification of novel targets for the N-terminal acetyltransferase NatB. *Eukaryot Cell* 5: 368-378

Pubmed: [Author and Title](#)

Google Scholar: [Author Only Title Only Author and Title](#)

Casey JP, Støve SI, McGorrian C, Galvin J, Blenski M, Dunne A, Ennis S, Brett F, King MD, Arnesen T, Lynch SA (2015) NAA10 mutation causing a novel intellectual disability syndrome with Long QT due to N-terminal acetyltransferase impairment. *Scientific Reports* 5: 16022

Pubmed: [Author and Title](#)

Google Scholar: [Author Only Title Only Author and Title](#)

Chen Z, Zhao P-X, Miao Z-Q, Qi G-F, Wang Z, Yuan Y, Ahmad N, Cao M-J, Hell R, Wirtz M, Xiang C-B (2019) SULTR3s Function in Chloroplast Sulfate Uptake and Affect ABA Biosynthesis and the Stress Response. *Plant Physiol* 180: 593-604

Pubmed: [Author and Title](#)

Google Scholar: [Author Only Title Only Author and Title](#)

Czechowski T, Stitt M, Altmann T, Udvardi MK, Scheible WR (2005) Genome-wide identification and testing of superior reference genes for transcript normalization in Arabidopsis. *Plant Physiol* 139: 5-17

Pubmed: [Author and Title](#)

Google Scholar: [Author Only Title Only Author and Title](#)

Dinh TV, Bienvenut WW, Linster E, Feldman-Salit A, Jung VA, Meinel T, Hell R, Giglione C, Wirtz M (2015) Molecular identification and functional characterization of the first Na-acetyltransferase in plastids by global acetylome profiling. *Proteomics* 15: 2426-2435

Pubmed: [Author and Title](#)

Google Scholar: [Author Only Title Only Author and Title](#)

Drazic A, Aksnes H, Marie M, Boczkowska M, Varland S, Timmerman E, Foyn H, Glomnes N, Rebowski G, Impens F, Gevaert K, Dominguez R, Arnesen T (2018) NAA80 is actin's N-terminal acetyltransferase and regulates cytoskeleton assembly and cell motility. *Proc Natl Acad Sci U S A*

Pubmed: [Author and Title](#)

Google Scholar: [Author Only Title Only Author and Title](#)

Dupree P, Sherrier DJ (1998) The plant Golgi apparatus. *Biochim Biophys Acta* 1404: 259-270

Pubmed: [Author and Title](#)

Google Scholar: [Author Only Title Only Author and Title](#)

Falb M, Aivaliotis M, Garcia-Rizo C, Bisle B, Tebbe A, Klein C, Konstantinidis K, Siedler F, Pfeiffer F, Oesterheld D (2006) Archaeal N-terminal protein maturation commonly involves N-terminal acetylation: a large-scale proteomics survey. *J Mol Biol* 362: 915-924

Pubmed: [Author and Title](#)

Google Scholar: [Author Only Title Only Author and Title](#)

Ferrandez-Ayela A, Micol-Ponce R, Sanchez-García AB, Alonso-Peral MM, Micol JL, Ponce MR (2013) Mutation of an Arabidopsis NatB N-Alpha-Terminal Acetylation Complex Component Causes Pleiotropic Developmental Defects. *PLoS ONE* 8: e80697, 80691-80611

Pubmed: [Author and Title](#)

Google Scholar: [Author Only Title Only Author and Title](#)

Frottin F, Martinez A, Peynot P, Mitra S, Holz RC, Giglione C, Meinel T (2006) The proteomics of N-terminal methionine cleavage. *Mol Cell Proteomics* 5: 2336-2349

Pubmed: [Author and Title](#)

Google Scholar: [Author Only Title Only Author and Title](#)

Giglione C, Fieulaine S, Meinel T (2015) N-terminal protein modifications: Bringing back into play the ribosome. *Biochimie*

Pubmed: [Author and Title](#)

Google Scholar: [Author Only Title Only Author and Title](#)

Heeg C, Kruse C, Jost R, Gutensohn M, Ruppert T, Wirtz M, Hell R (2008) Analysis of the Arabidopsis O-acetylserine(thiol)lyase gene family demonstrates compartment-specific differences in the regulation of cysteine synthesis. *Plant Cell* 20: 168-185

Pubmed: [Author and Title](#)

Google Scholar: [Author Only Title Only Author and Title](#)

Helbig AO, Rosati S, Pijnappel PW, van Breukelen B, Timmers MH, Mohammed S, Slijper M, Heck AJ (2010) Perturbation of the yeast N-acetyltransferase NatB induces elevation of protein phosphorylation levels. *BMC Genomics* 11: 685

Pubmed: [Author and Title](#)

Google Scholar: [Author Only Title Only Author and Title](#)

Hong H, Cai Y, Zhang S, Ding H, Wang H, Han A (2017) Molecular Basis of Substrate Specific Acetylation by N-Terminal Acetyltransferase NatB. *Structure* 25: 641-649 e643

Pubmed: [Author and Title](#)

Google Scholar: [Author Only Title Only Author and Title](#)

Huang da W, Sherman BT, Lempicki RA (2009a) Bioinformatics enrichment tools: paths toward the comprehensive functional analysis of large gene lists. *Nucleic Acids Res* 37: 1-13

Pubmed: [Author and Title](#)

Google Scholar: [Author Only Title Only Author and Title](#)

Huang da W, Sherman BT, Lempicki RA (2009b) Systematic and integrative analysis of large gene lists using DAVID bioinformatics resources. *Nat Protoc* 4: 44-57

Pubmed: [Author and Title](#)

Google Scholar: [Author Only Title Only Author and Title](#)

Kaundal R, Saini R, Zhao PX (2010) Combining Machine Learning and Homology-Based Approaches to Accurately Predict Subcellular Localization in Arabidopsis. *Plant Physiology* 154: 36-54

Pubmed: [Author and Title](#)

Google Scholar: [Author Only Title Only Author and Title](#)

Linster E, Stephan I, Bienvenut WW, Maple-Grodem J, Myklebust LM, Huber M, Reichelt M, Sticht C, Geir Moller S, Meinel T, Arnesen T, Giglione C, Hell R, Wirtz M (2015) Downregulation of N-terminal acetylation triggers ABA-mediated drought responses in Arabidopsis. *Nat Commun* 6: 7640

Pubmed: [Author and Title](#)

Google Scholar: [Author Only Title Only Author and Title](#)

Linster E, Wirtz M (2018) N-terminal acetylation: an essential protein modification emerges as an important regulator of stress responses. *J Exp Bot* 69: 4555-4568

Pubmed: [Author and Title](#)

Google Scholar: [Author Only Title Only Author and Title](#)

Nguyen KT, Kim JM, Park SE, Hwang CS (2019) N-terminal methionine excision of proteins creates tertiary destabilizing N-degrons of the Arg/N-end rule pathway. *J Biol Chem* 294: 4464-4476

Pubmed: [Author and Title](#)

Google Scholar: [Author Only Title Only Author and Title](#)

Nilsson OB, Hedman R, Marino J, Wickles S, Bischoff L, Johansson M, Muller-Lucks A, Trovato F, Puglisi JD, O'Brien EP, Beckmann R, von Heijne G (2015) Cotranslational Protein Folding inside the Ribosome Exit Tunnel. *Cell Rep* 12: 1533-1540

Pubmed: [Author and Title](#)

Google Scholar: [Author Only Title Only Author and Title](#)

Noji M, Inoue K, Kimura N, Gouda A, Saito K (1998) Isoform-dependent differences in feedback regulation and subcellular localization of serine acetyltransferase involved in cysteine biosynthesis from Arabidopsis thaliana. *J Biol Chem* 273: 32739-32745

Pubmed: [Author and Title](#)

Google Scholar: [Author Only Title Only Author and Title](#)

Pesaresi P, Gardner NA, Masiero S, Dietzmann A, Eichacker L, Wickner R, Salamini F, Leister D (2003) Cytoplasmic N-terminal protein acetylation is required for efficient photosynthesis in Arabidopsis. *Plant Cell* 15: 1817-1832

Pubmed: [Author and Title](#)

Google Scholar: [Author Only Title Only Author and Title](#)

Pierre M, Traverso JA, Boisson B, Domenichini S, Bouchez D, Giglione C, Meinel T (2007) N-myristoylation regulates the SnRK1 pathway in Arabidopsis. *Plant Cell* 19: 2804-2821

Pubmed: [Author and Title](#)

Google Scholar: [Author Only Title Only Author and Title](#)

Polevoda B, Arnesen T, Sherman F (2009) A synopsis of eukaryotic N-terminal acetyltransferases: nomenclature, subunits and substrates. *BMC Proc* 3 Suppl 6: S2

Pubmed: [Author and Title](#)

Google Scholar: [Author Only Title Only Author and Title](#)

Polevoda B, Brown S, Cardillo TS, Rigby S, Sherman F (2008) Yeast N(alpha)-terminal acetyltransferases are associated with ribosomes. *J Cell Biochem* 103: 492-508

Pubmed: [Author and Title](#)

Google Scholar: [Author Only Title Only Author and Title](#)

Polevoda B, Cardillo TS, Doyle TC, Bedi GS, Sherman F (2003) Nat3p and Mdm20p are required for function of yeast NatB Nalpha-terminal acetyltransferase and of actin and tropomyosin. J Biol Chem 278: 30686-30697

Pubmed: [Author and Title](#)

Google Scholar: [Author Only Title Only Author and Title](#)

Polevoda B, Sherman F (2003) N-terminal acetyltransferases and sequence requirements for N-terminal acetylation of eukaryotic proteins. J Mol Biol 325: 595-622

Pubmed: [Author and Title](#)

Google Scholar: [Author Only Title Only Author and Title](#)

Ree R, Myklebust LM, Thiel P, Foyn H, Fladmark KE, Arnesen T (2015) The N-terminal acetyltransferase Naa10 is essential for zebrafish development. Biosci Rep 35

Pubmed: [Author and Title](#)

Google Scholar: [Author Only Title Only Author and Title](#)

Reid DW, Nicchitta CV (2015) Diversity and selectivity in mRNA translation on the endoplasmic reticulum. Nature reviews. Molecular cell biology 16: 221-231

Pubmed: [Author and Title](#)

Google Scholar: [Author Only Title Only Author and Title](#)

Rosso MG, Li Y, Strizhov N, Reiss B, Dekker K, Weisshaar B (2003) An Arabidopsis thaliana T-DNA mutagenized population (GABI-Kat) for flanking sequence tag-based reverse genetics. Plant Mol Biol 53: 247-259

Pubmed: [Author and Title](#)

Google Scholar: [Author Only Title Only Author and Title](#)

Sessions A, Burke E, Presting G, Aux G, McElver J, Patton D, Dietrich B, Ho P, Bacwaden J, Ko C, Clarke JD, Cotton D, Bullis D, Snell J, Miguel T, Hutchison D, Kimmerly B, Mitzel T, Katagiri F, Glazebrook J, Law M, Goff SA (2002) A high-throughput Arabidopsis reverse genetics system. Plant Cell 14: 2985-2994

Pubmed: [Author and Title](#)

Google Scholar: [Author Only Title Only Author and Title](#)

Singer JM, Shaw JM (2003) Mdm20 protein functions with Nat3 protein to acetylate Tpm1 protein and regulate tropomyosin-actin interactions in budding yeast. Proc Natl Acad Sci U S A 100: 7644-7649

Pubmed: [Author and Title](#)

Google Scholar: [Author Only Title Only Author and Title](#)

Starheim KK, Arnesen T, Gromyko D, Rynningen A, Varhaug JE, Lillehaug JR (2008) Identification of the human N(alpha)-acetyltransferase complex B (hNatB): a complex important for cell-cycle progression. Biochem J 415: 325-331

Pubmed: [Author and Title](#)

Google Scholar: [Author Only Title Only Author and Title](#)

Van Damme P, Lasa M, Polevoda B, Gazquez C, Elosegui-Artola A, Kim DS, De Juan-Pardo E, Demeyer K, Hole K, Larrea E, Timmerman E, Prieto J, Arnesen T, Sherman F, Gevaert K, Aldabe R (2012) N-terminal acetylome analyses and functional insights of the N-terminal acetyltransferase NatB. Proc Natl Acad Sci U S A 109: 12449-12454

Pubmed: [Author and Title](#)

Google Scholar: [Author Only Title Only Author and Title](#)

Xu F, Huang Y, Li L, Gannon P, Linster E, Huber M, Kapos P, Bienvenut W, Polevoda B, Meinnel T, Hell R, Giglione C, Zhang Y, Wirtz M, Chen S, Li X (2015) Two N-terminal acetyltransferases antagonistically regulate the stability of a nod-like receptor in Arabidopsis. Plant Cell 27: 1547-1562

Pubmed: [Author and Title](#)

Google Scholar: [Author Only Title Only Author and Title](#)